Low-Frequency Noise in Low-Dimensional van der Waals Materials

Alexander A. Balandin
Department of Electrical Engineering and
Materials Science and Engineering Program
University of California – Riverside, USA

Sergey Rumyantsev
Institute of High-Pressure Physics
Polish Academy of Sciences
Warsaw, Poland

ICNF – 2019: Neuchâtel, Switzerland

UC RIVERSIDE UNIVERSITY OF CALIFORNIA

City of Riverside

UCR Botanic Gardens

UCR Bell Tower

Joshua Tree Park

UCR Engineering Building

Areas of Expertise

Graphene, Phonons and Thermal Properties

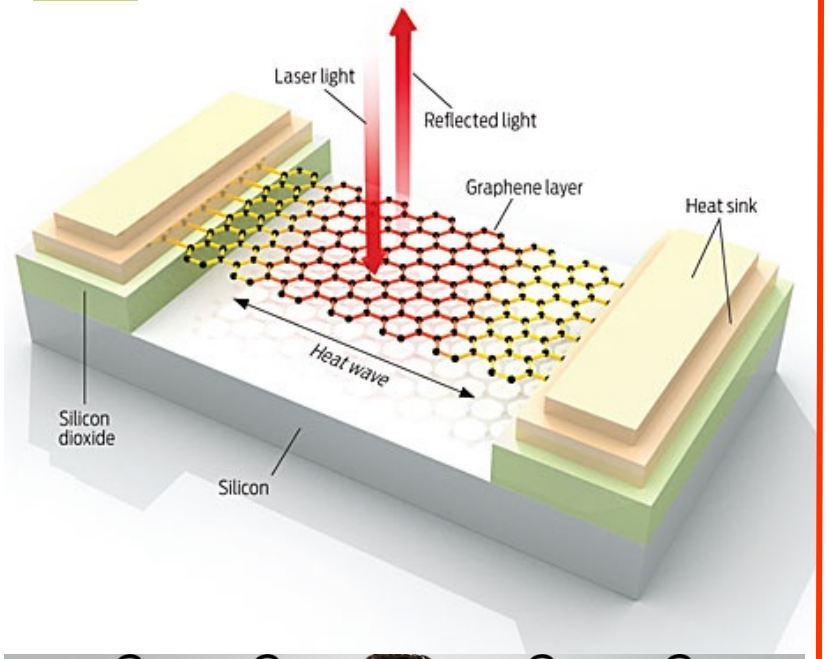

2D/1D Materials and Devices, and Low-Frequency Noise

nature nanotechnology
PROGRESS ARTICLE
PUBLISHED ONLINE: 5 AUGUST 2013 | DOI: 10.1038/NNANO.2013.144

Low-frequency 1/*f* noise in graphene devices

Alexander A. Balandin

Low-frequency noise with a spectral density that depends inversely on frequency has been observed in a wide variety of systems including current fluctuations in resistors, intensity fluctuations in music and signals in human cognition. In electronics, the phenomenon, which is known as 1/*f* noise, flicker noise or excess noise, hampers the operation of numerous devices and circuits, and can be a significant impediment to the development of practical applications from new materials. Graphene offers unique opportunities for studying 1/*f* noise because of its two-dimensional structure and widely tunable two-dimensional carrier concentration. The creation of practical graphene-based devices will also depend on our ability to understand and control the low-frequency noise in this material system. Here, the characteristic features of 1/*f* noise in graphene and few-layer graphene are reviewed, and the implications of such noise for the development of graphene-based electronics including high-frequency devices and sensors are examined.

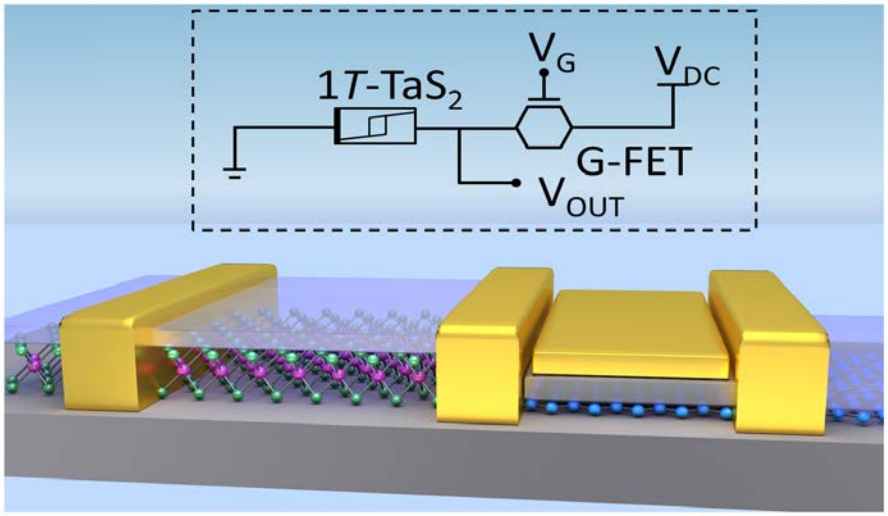

Outline

- → Introduction
- → Noise Experiments with Graphene
  - → Graphene under irradiation
  - → Noise as signal in graphene sensors
- → Noise in 2D CDW Devices
  - → 2D charge-density-waves
  - → Noise spectroscopy of CDWs
  - → Radiation hardness of 2D CDW devices
- → Quasi-1D van der Waals Materials
  - → Interconnect applications of 1D metals
  - → Unusual noise characteristics in 1D
- → Conclusions

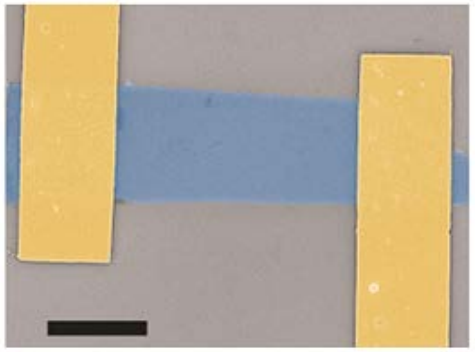

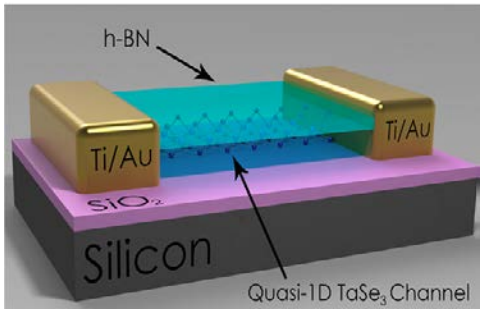

Nano-Device Laboratory

Terminology: Van der Waals Materials

From quasi-2D to quasi-1D

Graphene

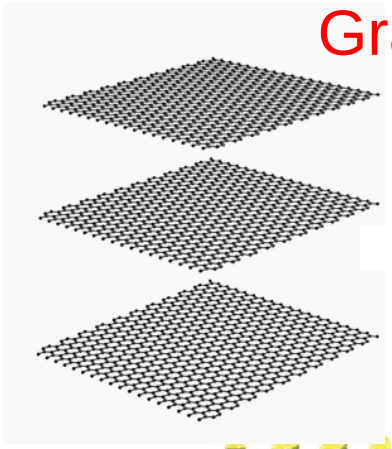

MoS_2

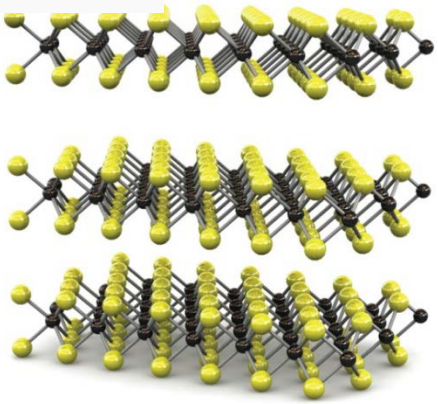

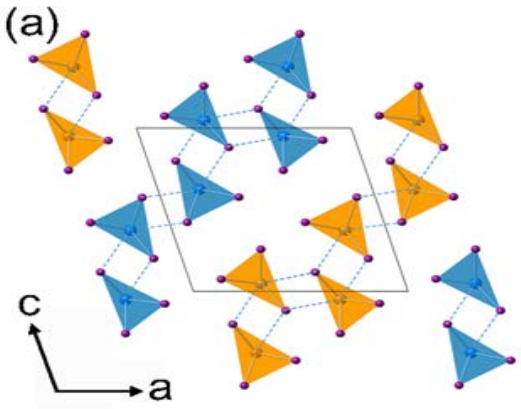

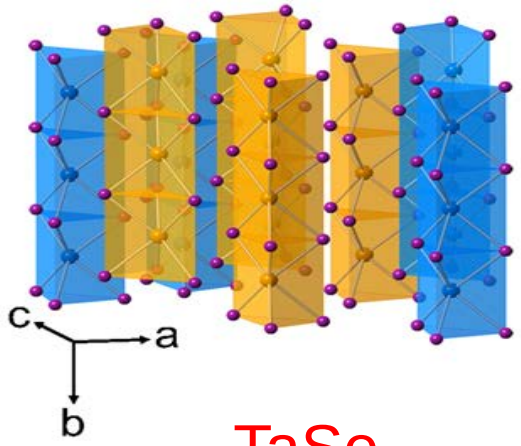

$TaSe_3$

→ Crystal structure of monoclinic $TaSe_3$, with alternating layers of $TaSe_3$

→ Cross section of the unit cell, perpendicular to the chain axis (b axis).

→ The side view: 1D nature of $TaSe_3$ chains along the b axis.

Part – I: Noise in Graphene

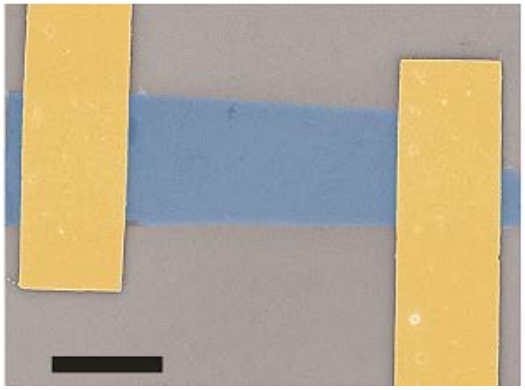

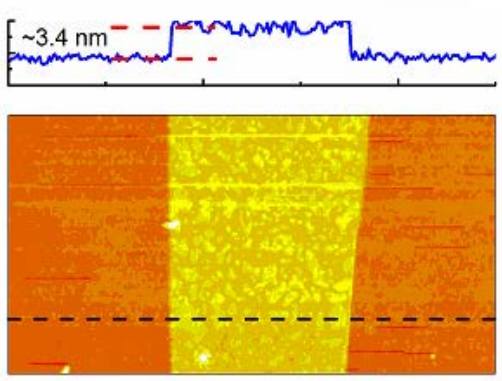

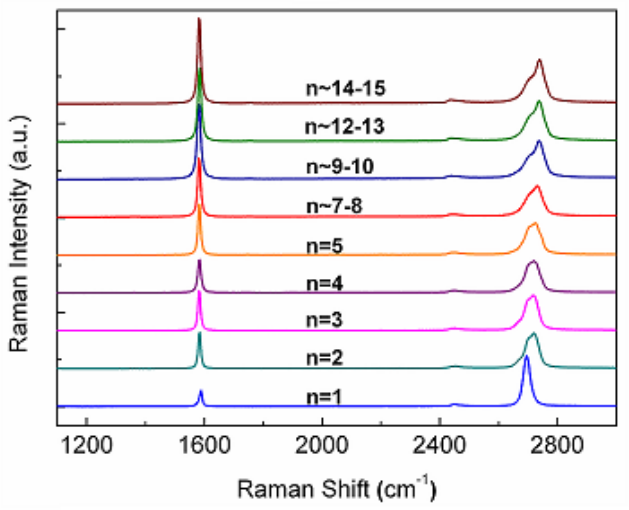

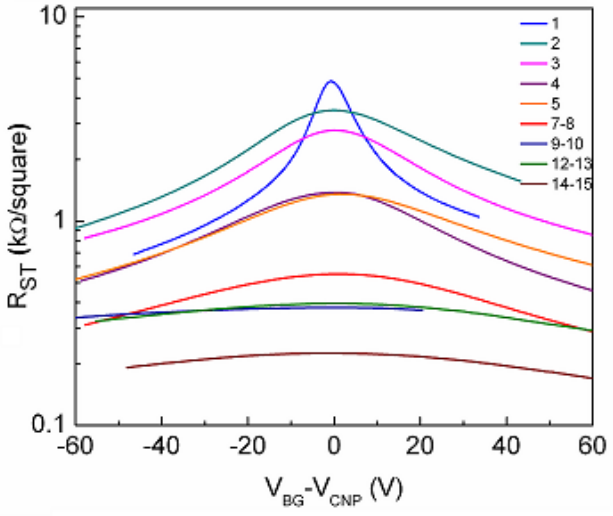

- → Practical task of noise scaling with the thickness
- → Possibility of addressing an old problem of origin of noise: surface vs. volume

The back-gated devices were fabricated by the electron-beam lithography with Ti/Au (6-nm/60-nm) electrodes.

R_{ST} is sheet resistance

Graphene channel area A varied from 1.5 to 70 μm^2

Electronic Noise in Graphene Devices

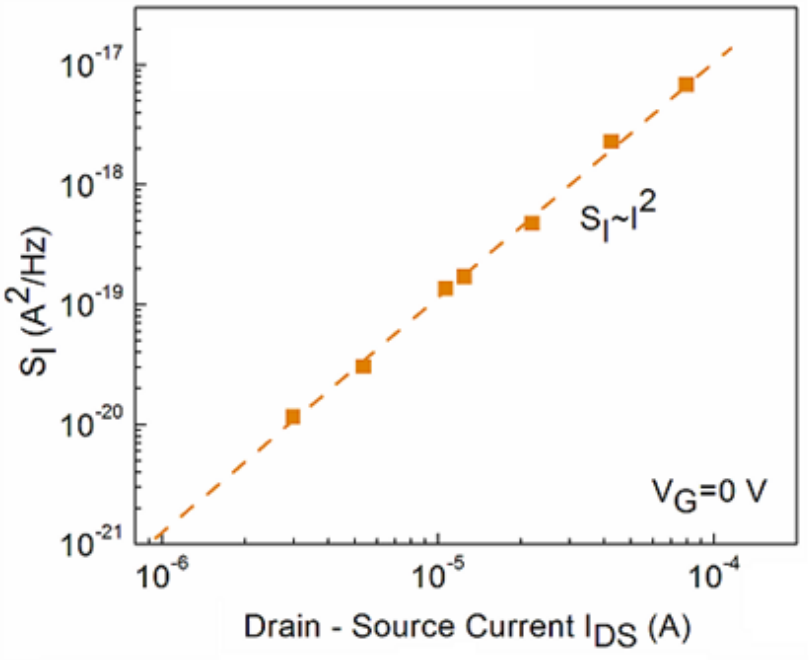

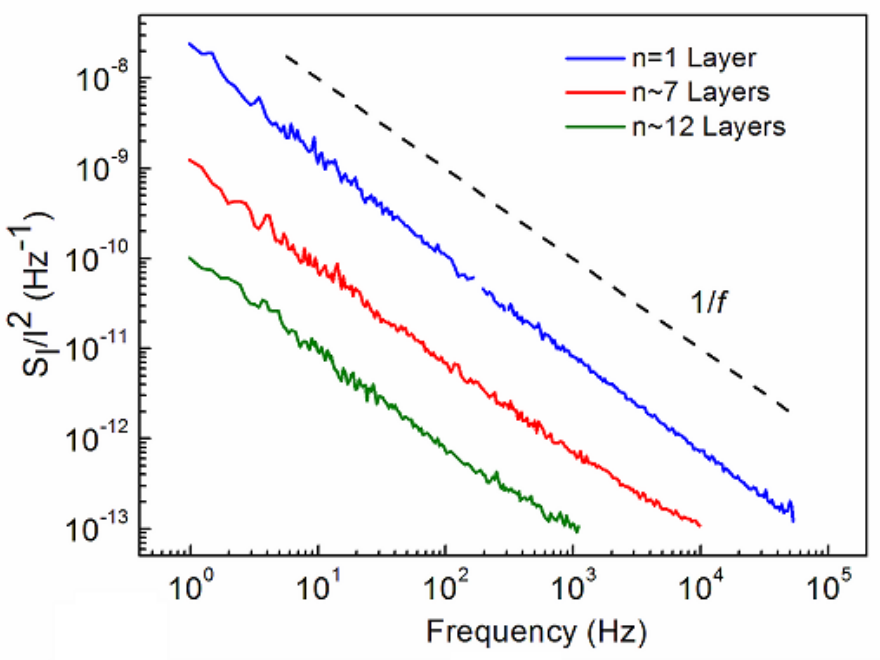

To minimize the influence of the contact resistance, most of the noise measurements were performed close to CNP.

G. Liu, S. Rumyantsev, M. S. Shur, and A. A. Balandin, "Origin of 1/ f noise in graphene multilayers: surface vs. volume," Appl. Phys. Lett., **102**, 93111 (2013).

Old Question: Surface vs. Volume Effect

The intensity of discussions can be inferred even from the titles of seminal publications on the subject: "1/*f* noise is no surface effect" (1969)[9] followed by "1/*f* noise: still a surface effect" (1972).[10]

[9]F. N. Hooge, Phys. Lett. A **29**, 139 (1969).
[10]A. Mircea, A. Roussel, and A. Mitonneau, Phys. Lett. A **41**, 345 (1972).

→ 1/f noise is dominated by the volume noise when the thickness exceeds ~7 atomic layers (~2.5 nm).

→ The 1/f noise is the surface phenomenon below this thickness.

Mechanism of 1/*f* Noise in Electronic Materials and Devices

$$I \sim qN\mu$$

$$\delta I \sim q(\delta N)\mu + qN(\delta\mu)$$

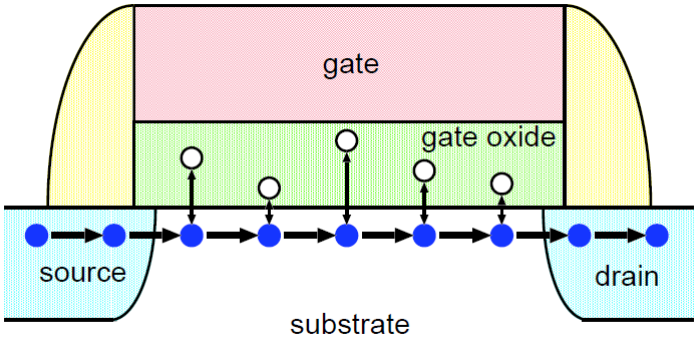

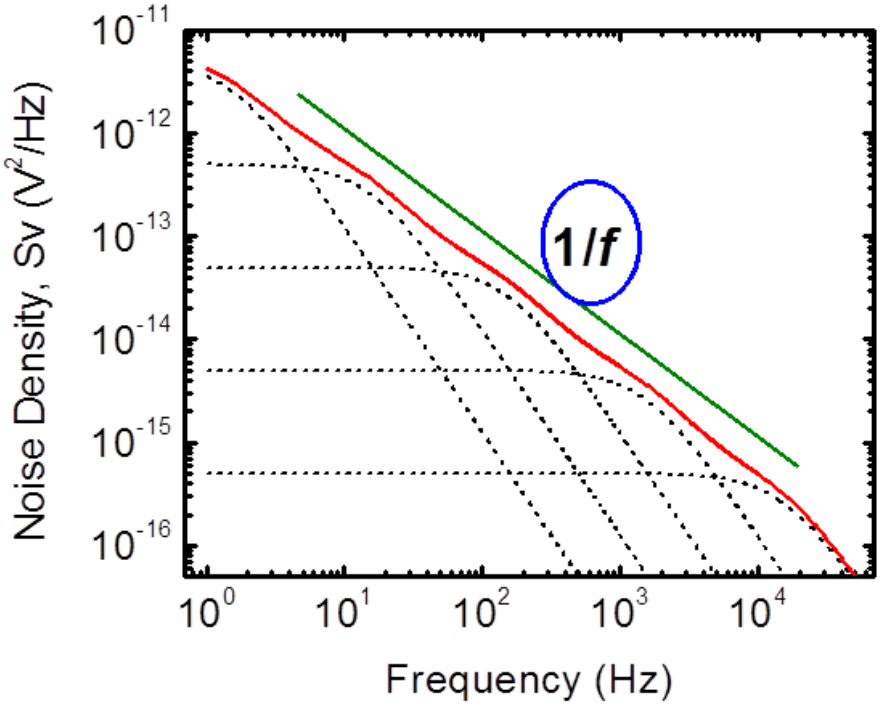

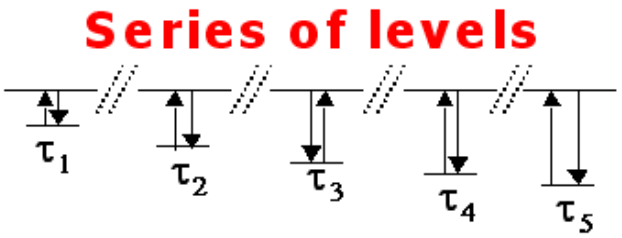

McWhorter's model: $g(\tau_N) = [\tau_N \ln(\tau_2/\tau_1)]^{-1}$

$$S_N(\omega) = 4\overline{\delta N^2}\int_{\tau_1}^{\tau_2} g(\tau_N)\frac{\tau_N}{1+(\omega\tau_N)^2}d\tau_N$$

Specifics of Electronic Noise in Graphene

$$A = (1/N)\Sigma_{m=1}^{N} f_m S_{I_m} / I_m^2$$

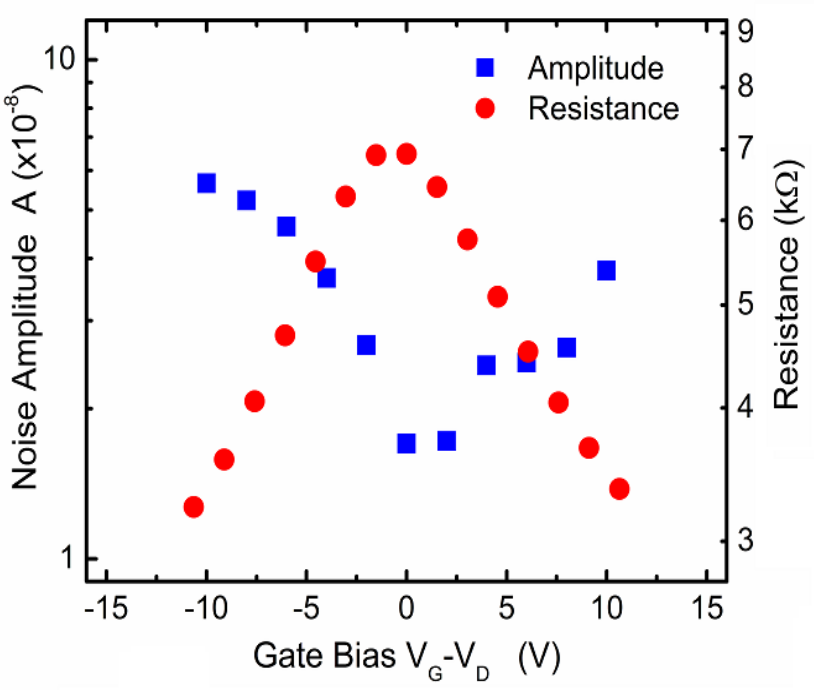

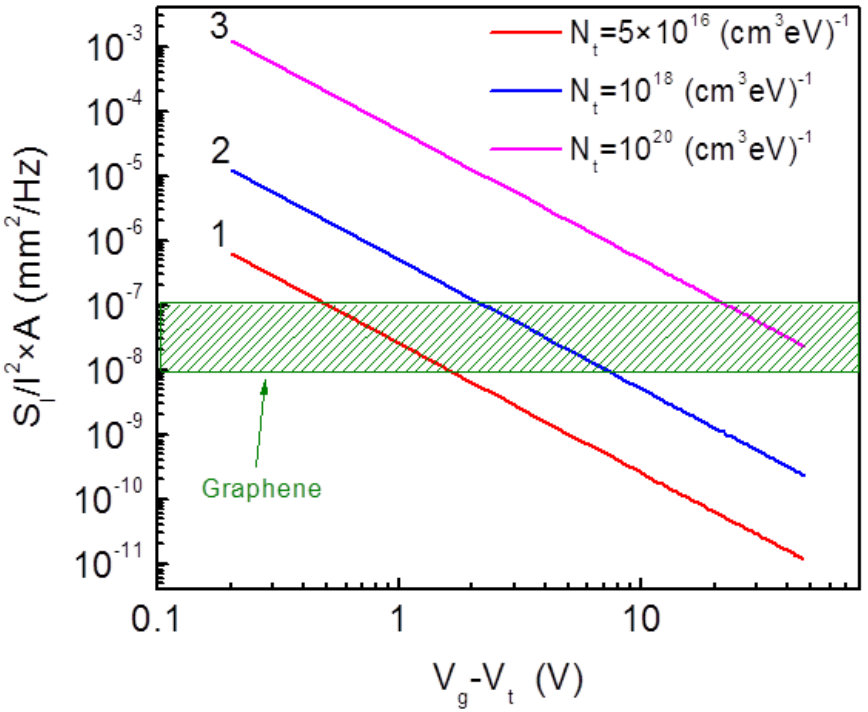

In some graphene devices, V-shape becomes M-shape dependence at lager bias range

S_I/I^2 =10^{-9} to 10^{-7} Hz^{-1} at f=10 Hz or A=10^{-9} – 10^{-7}

$(S_I/I^2)L\times W$ =10^{-8} – 10^{-7} μm²/Hz

Investigation of 1/*f* Noise in Graphene Devices under Irradiation

Goal

Controlled introduction of defects by electron beam irradiation and observation of the evolution of 1/f noise level

Methodology

Step I: Raman of pristine graphene
Step II: IV characteristics and noise measurements
Step III: E-beam irradiation of the device
Step III: Raman of the irradiated device
Step IV: IV characteristics and noise measurements

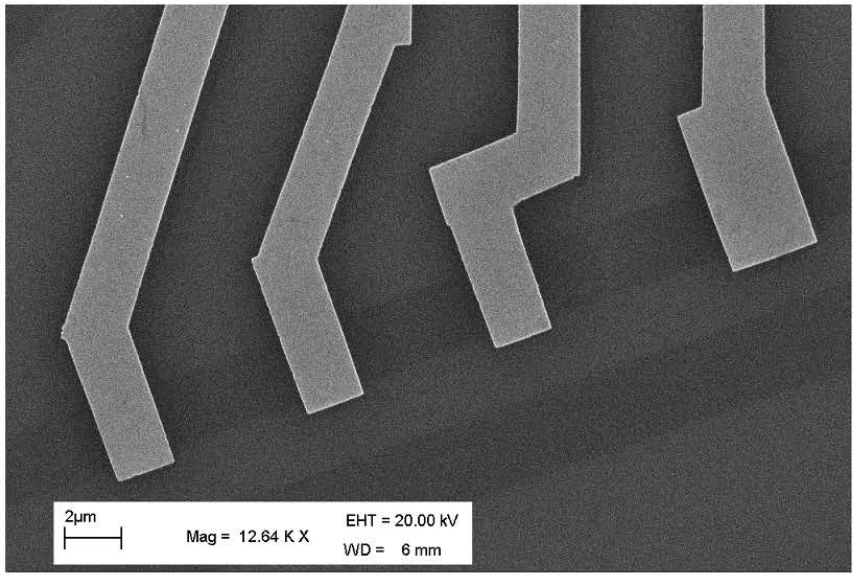

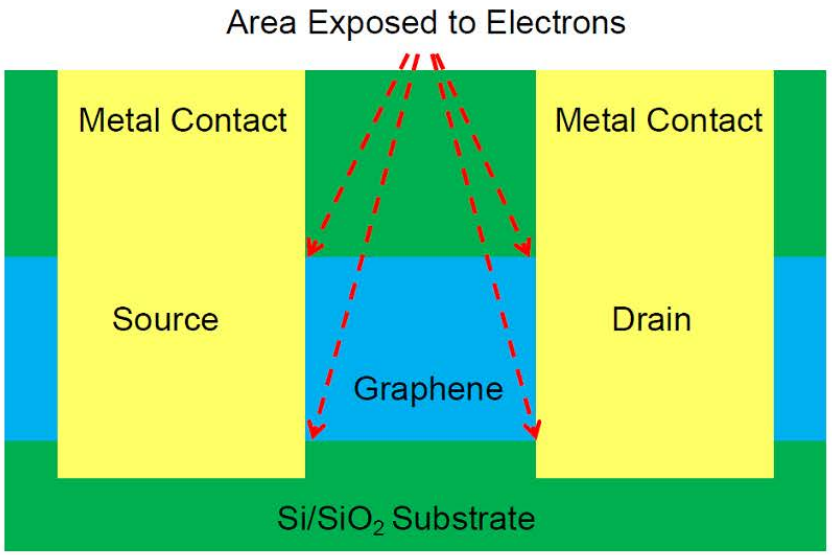

Introduction of Structural Defects to Graphene by Electron Beam Irradiation

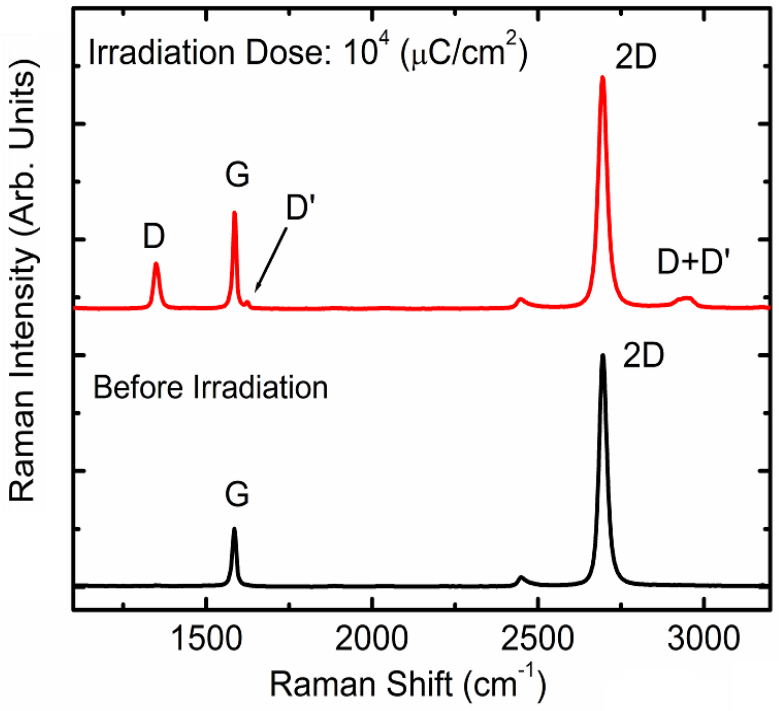

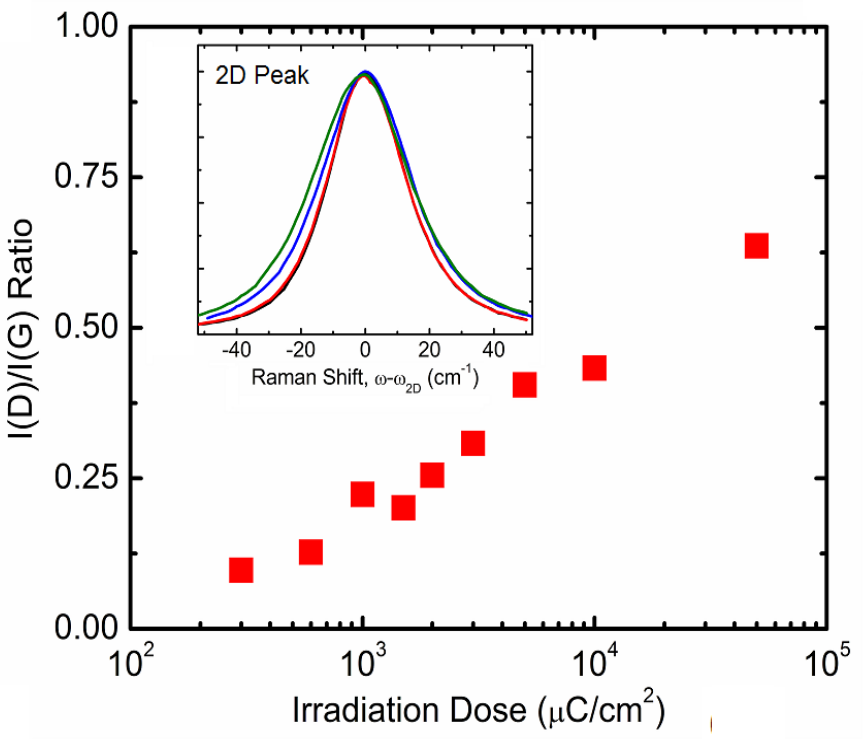

The electron energy was set to 20 keV in order to exclude the severe knock-on damage to the graphene crystal lattice, which starts at ~50 keV

Electron Beam Irradiation Effects on Electronic Properties of Graphene

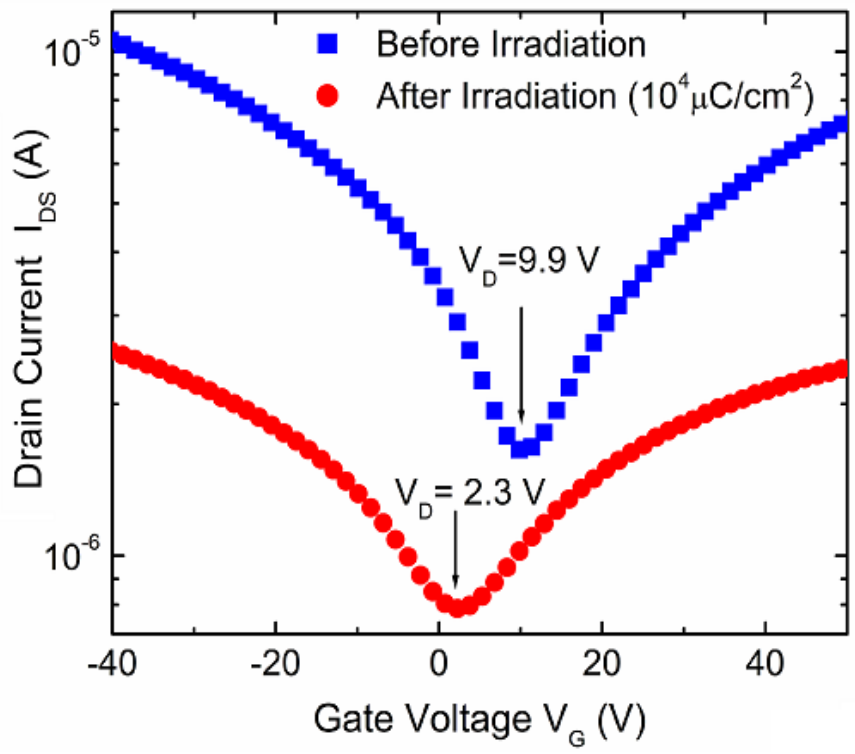

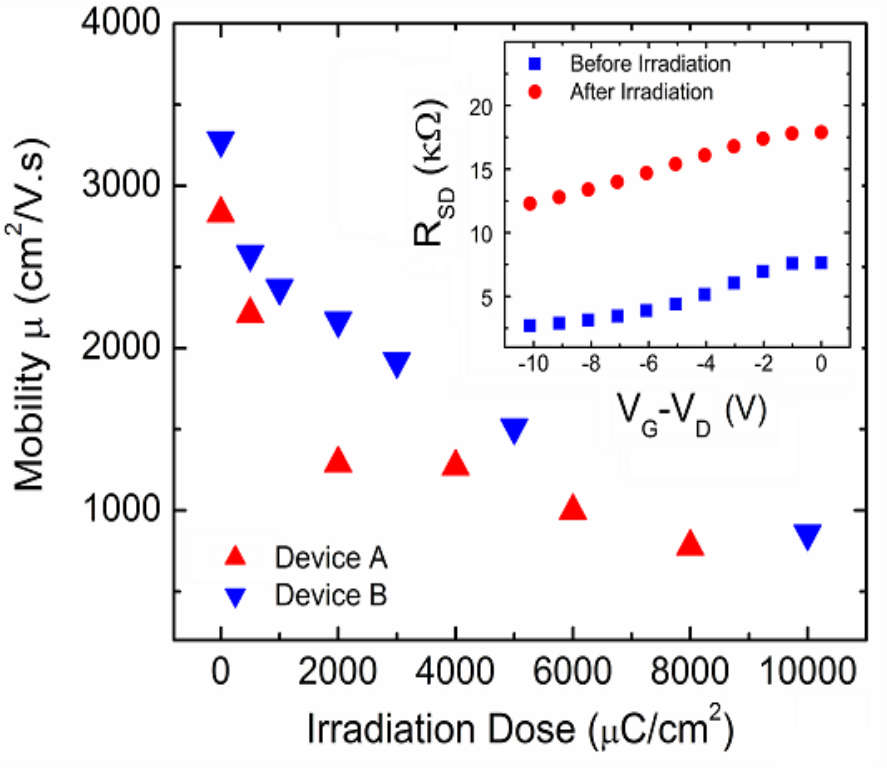

The Dirac point shift to negative side was observed for most devices, although in a very few cases, we recorded a positive shift after some irradiation steps.

Electronic Noise Suppression via Electron Beam Irradiation

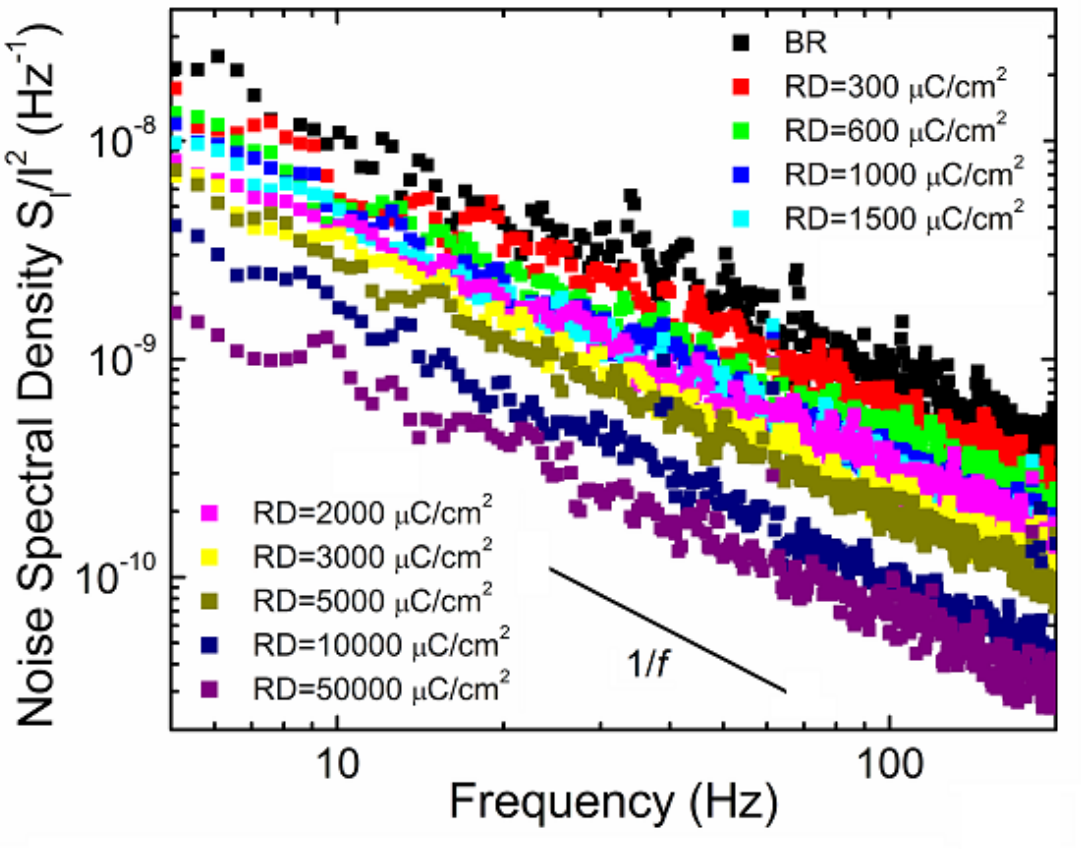

The noise was measured in the linear region of the drain bias keeping the source at a ground potential.

The flicker 1/*f* noise is usually associated with structural defects.

Introduction of defects by irradiation normally results in increased 1/*f* noise and reduced mobility

M.Z. Hossain, S. Rumyantsev, M.S. Shur and A.A. Balandin, "Reduction of 1/f noise in graphene after electron-beam irradiation," *Applied Physics Letters*, **102**, 153512 (2013).

Low-Frequency Noise Suppression via Electron Beam Irradiation

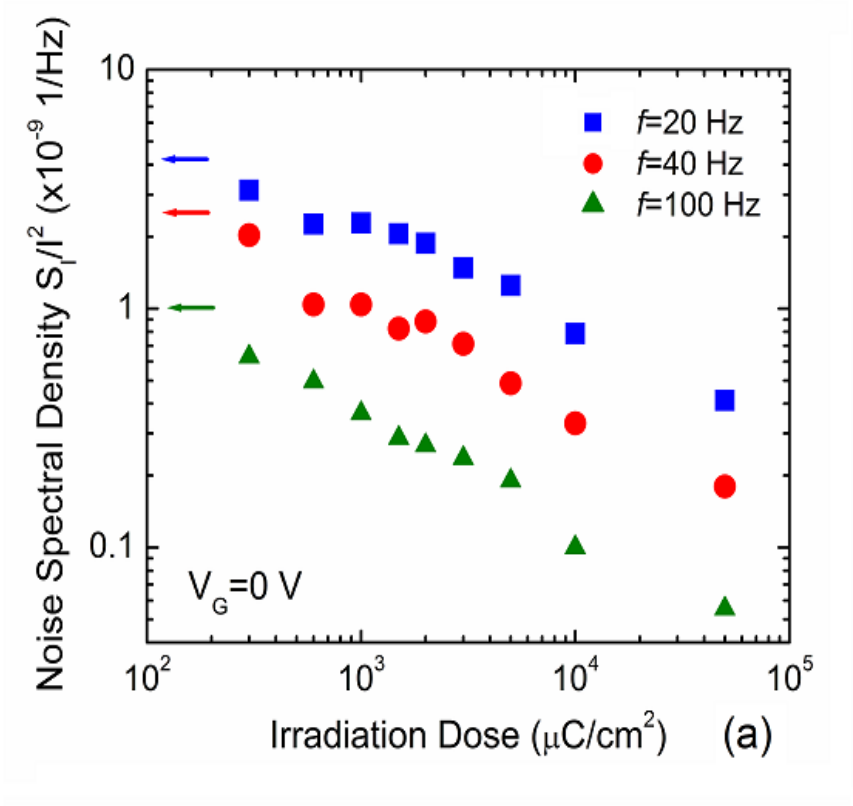

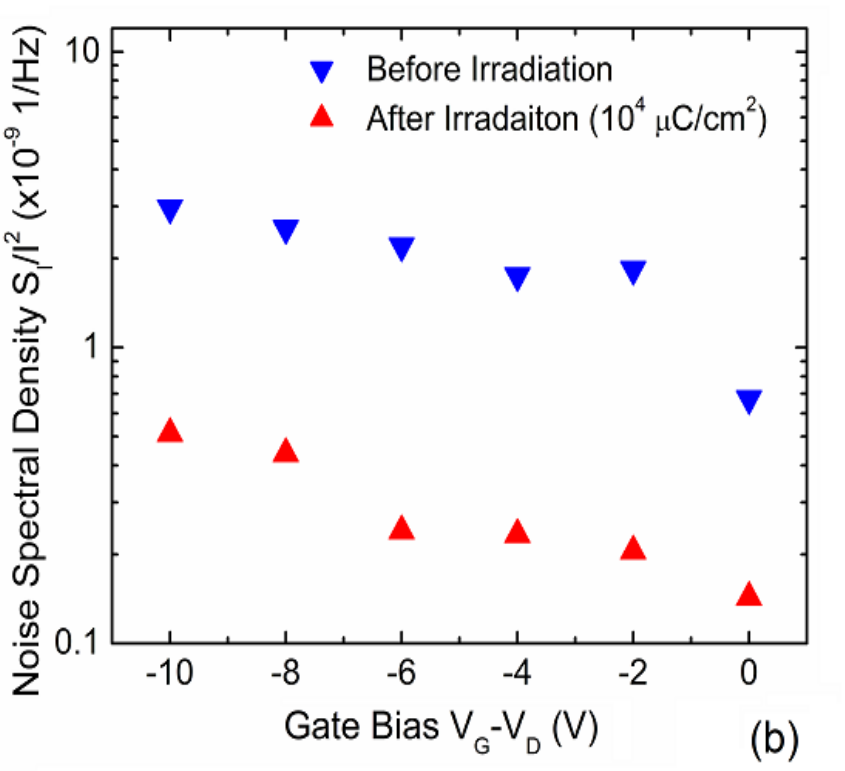

Noise reduces monotonically with the increasing R_D for the entire range of negative gate-bias voltages, V_G-V_D. The same trend was observed for the positive gate bias.

Possible Mechanisms of the 1/*f* Noise and its Suppression in Graphene

McWhorter model of the number of carriers fluctuations:

$$\frac{S_I}{I^2} = \frac{\lambda k T N_t}{f A V n^2}$$

→ N_t is the concentration of the traps near the E_F responsible for noise
→ A is the gate area
→ n is the carriers concentrations
→ λ is the tunneling constant

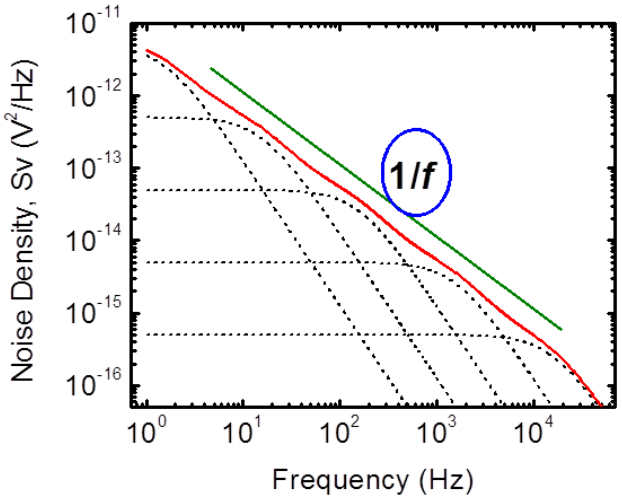

Yu. M. Galperin, V. G. Karpov, and V. I. Kozub, Sov. Phys. JETP, 68, 648 (1989).

A. P. Dmitriev, M. E. Levinshtein, and S. L. Rumyantsev, J. Appl. Phys., 106, 024514 (2009).

→ N_t is not the total concentration of traps!

→ Reduction in N_t after irradiation? – possible but unlikely

$$g(\tau_N) = [\tau_N \ln(\tau_2/\tau_1)]^{-1}$$

$$S_N(\omega) = 4\overline{\delta N^2}\int_{\tau_1}^{\tau_2} g(\tau_N)\frac{\tau_N}{1+(\omega\tau_N)^2}d\tau_N$$

Possible Mechanisms of the 1/*f* Noise in Graphene

Noise spectral density of the elementary fluctuation in the mobility fluctuation model:

$$\frac{S_I}{I^2} \propto \frac{N_t^{\mu}}{V} \frac{\tau\varsigma(1-\varsigma)}{1+(\omega\tau)^2} l_0^2 (\sigma_2 - \sigma_1)^2$$

- → $N_{t\mu}$ is concentration of the scattering centers contributing to 1/*f* noise
- → l_0 is MFP of the charge carriers
- → ζ is the probability for a scattering center to be in the state with the cross-section σ_1

Yu. M. Galperin, V.G. Karpov, V.I Kozub, *Sov. Phys. JETP* **68**, 648–653 (1989).

Yu. M. Galperin, V.L. Gurevich and V.I. Kozub, *Europhys. Lett.* **10,** 753–758 (1989).

A.P. Dmitriev, M.E. Levinshtein, S.L. Rumyantsev, *J. Appl. Phys.* **106,** 024514 (2009).

Independent Confirmation:

Ting Wu, et al., Low-frequency noise in irradiated graphene FETs, Appl. Phys. Lett. 113, 193502 (2018)

→ $N_{t\mu}$ may change during the irradiation or may stay about the same

→ N_t that limit electron mobility increases

→ Noise is defined by the electron MFP: S_I/I^2 ($\sim l_0^2$)

→ Reduced mobility results in reduced MFP

→ In graphene μ is limited by the scattering from charged defects even at RT

Low-Frequency Fluctuations as a Signal Rather then Noise

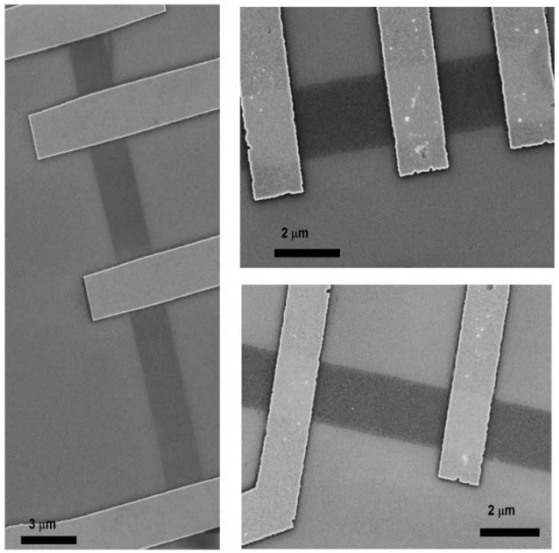

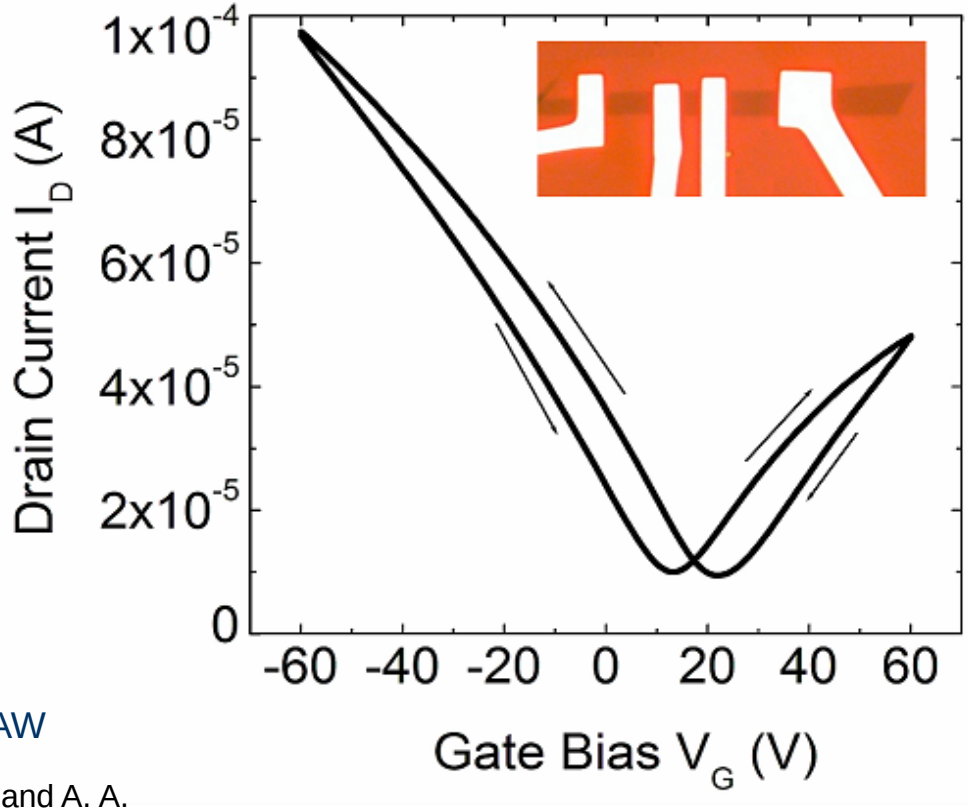

→High gas sensitivity (<1 ppb); Linear response to the gas concentration

→ Sensing parameters: change in resistivity; shift in Dirac point voltage; frequency of SAW

S. Rumyantsev, G. Liu, M. S. Shur, R. A. Potyrailo, and A. A. Balandin, "Selective gas sensing with a single pristine graphene transistor," Nano Lett.,12, 2294 (2012).

Look for G-R bulges, which can be informative → sensor selectivity

Generation – Recombination Bulges in Spectrum of Graphene under Gas Exposure

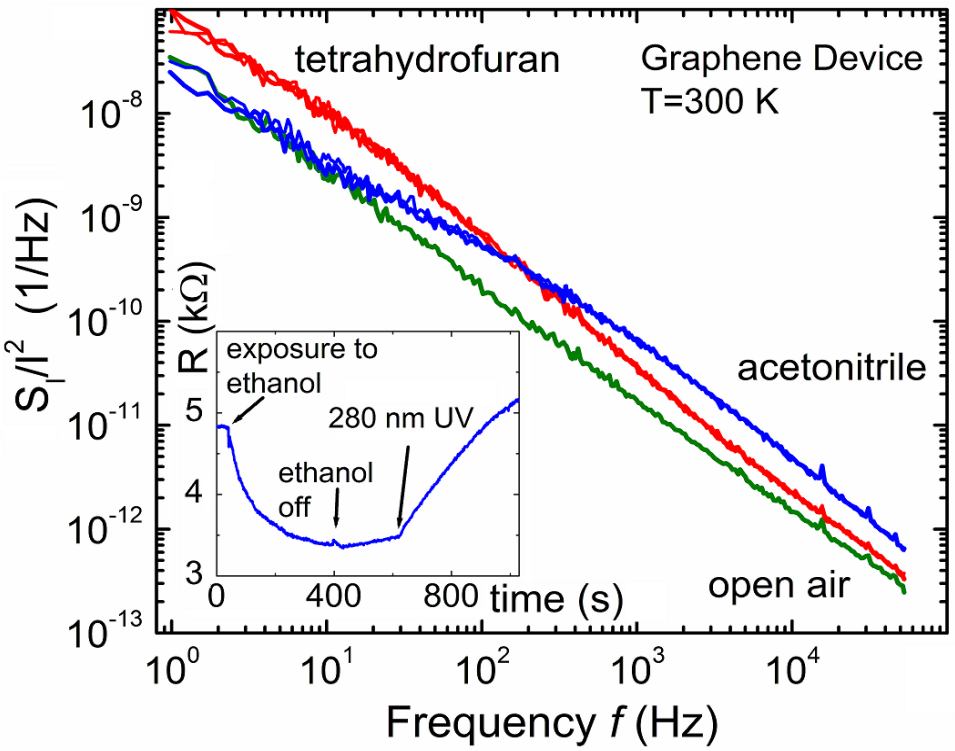

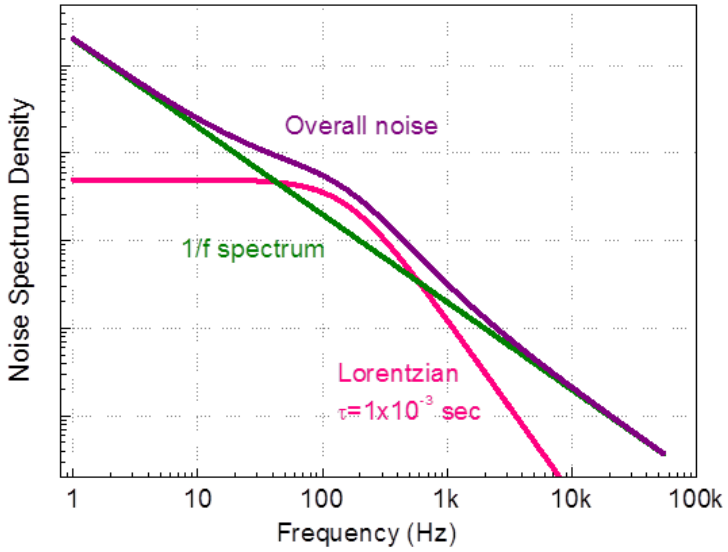

Superposition of a Lorentzian noise with defined relaxation time on a 1/f noise results in a bulge with specific frequency $S \propto \frac{1}{1+(\omega\tau)^2}$

→ Vapors generated by bubbling dry carrier gas - air – through solvent and diluting the gas flow with dry carrier gas
→ Vapors generated at ~0.5 P/P_o, where P during the experiment and P_o is the saturated vapor pressure
→ Measurements performed at V_G=0 V ("hole" region of graphene I-V)
→ The contact resistance per unit width: 0.2 – 2.0 Ω-mm

Reproducibility of G-R Bulges in Spectrum of Graphene under Vapor and Gas Exposure

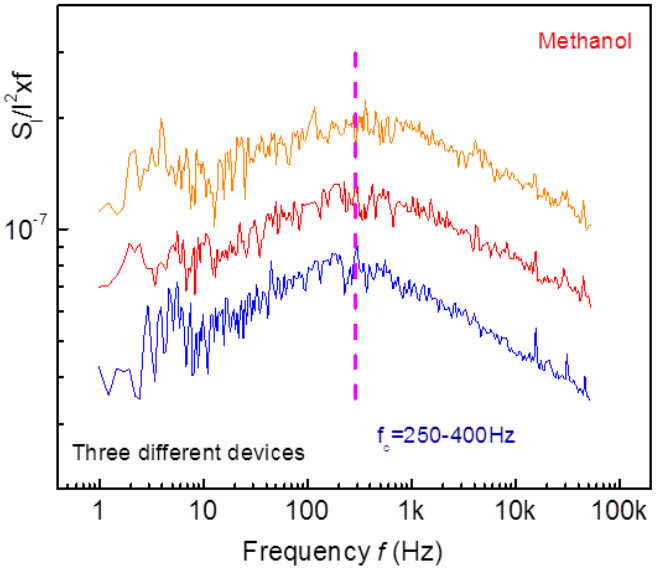

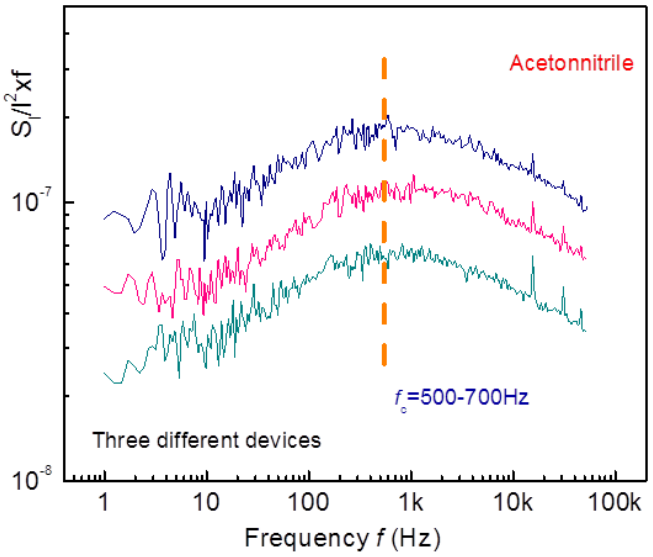

- The characteristics frequency f_c of Lorentzian peaks with certain vapor gases is reproducible for different graphene devices
- The gas molecules can create specific traps and scattering centers in graphene, which lead to either number of carriers fluctuation due to the fluctuations of traps occupancy or to the mobility fluctuations due to fluctuations of the scattering cross sections

S. Rumyantsev, G. Liu, M. S. Shur, R. A. Potyrailo, and A. A. Balandin, “Selective gas sensing with a single pristine graphene transistor,” Nano Lett.,12, 2294 (2012).

Part – II: Noise of Charge Density Waves

Normal state $T > T_c$

Electron Density $\rho_e = const$

Atomic Spacing a

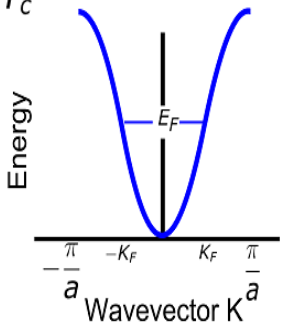

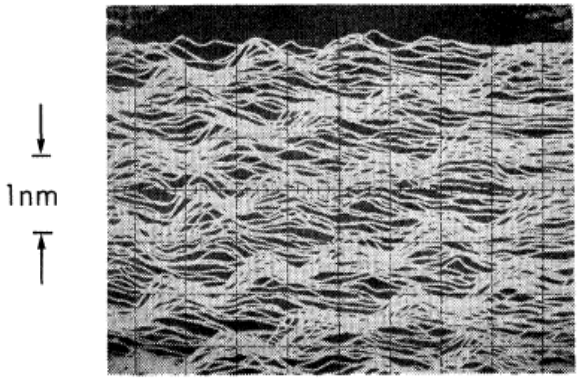

Peierls state $T < T_c$

Electron Density $\rho_e = \rho_0 + \rho_1 cos(qx + \lambda_c)$

λ_c

Atomic Spacing

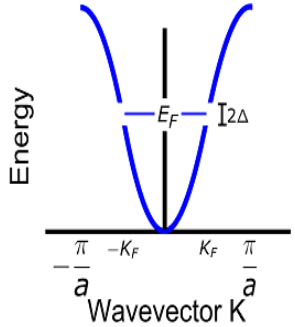

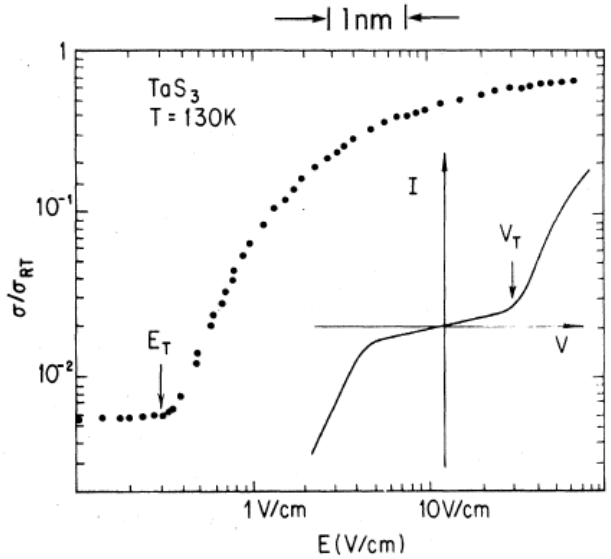

G. Gruner, Rev. Mod. Phys., **60**, 1129 (1988).
R.V. Coleman, *Phys. Rev. Lett.*, **55**, 394 (1985

CDW Effects in 1T-TaS_2

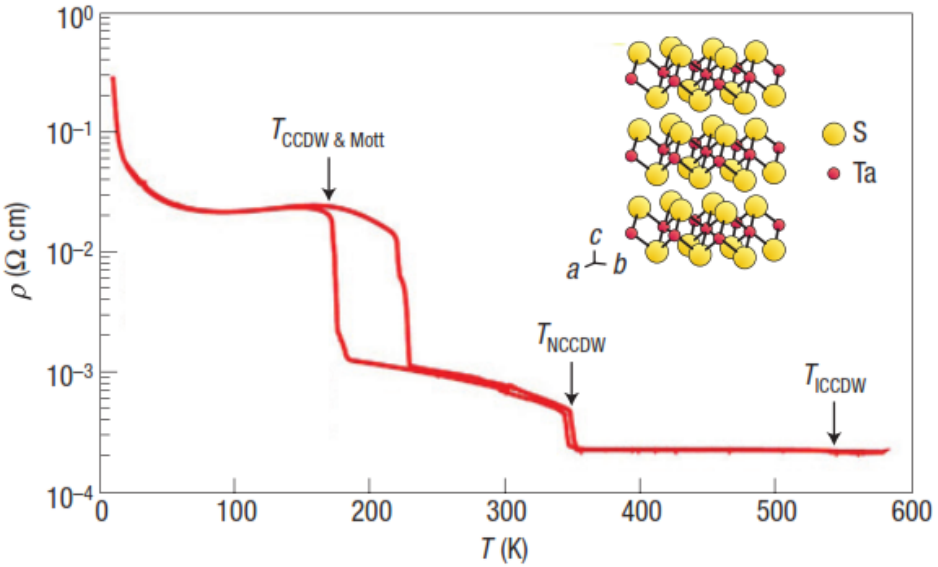

B. Sipos et al, Nature Mat., 7, 960 (2008)

- → 1T-TaS_2 experiences several CDW transitions
- → CDW phase transition is accompanied by an abrupt resistance change
- → C-CDW to NC-CDW transition (~180 K) appears in thick film but absent in thin films (H<9 nm)
- → NC-CDW to IC-CDW phase transition at 350-360 K is preserved as the thickness reduced

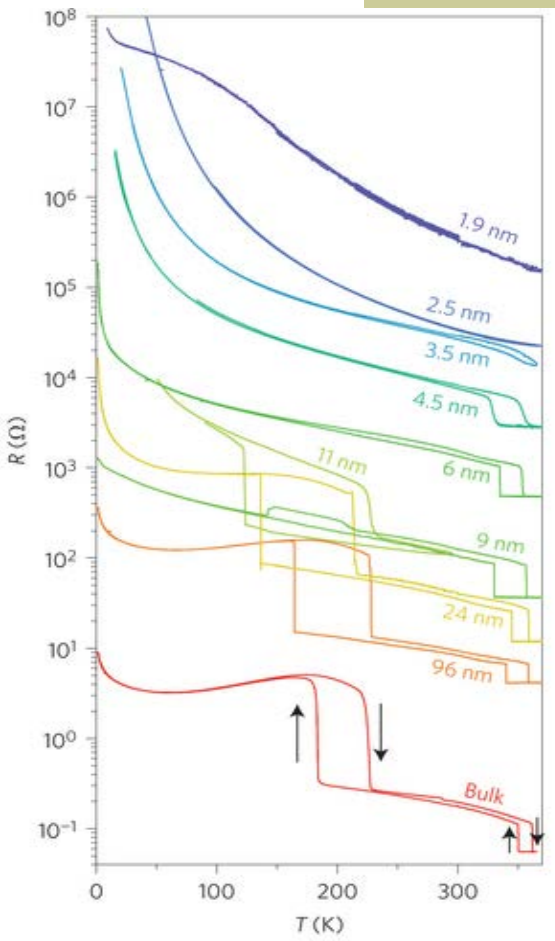

Y. Yu et al, Nature Nanotech (2015)

2D Charge-Density-Wave Devices

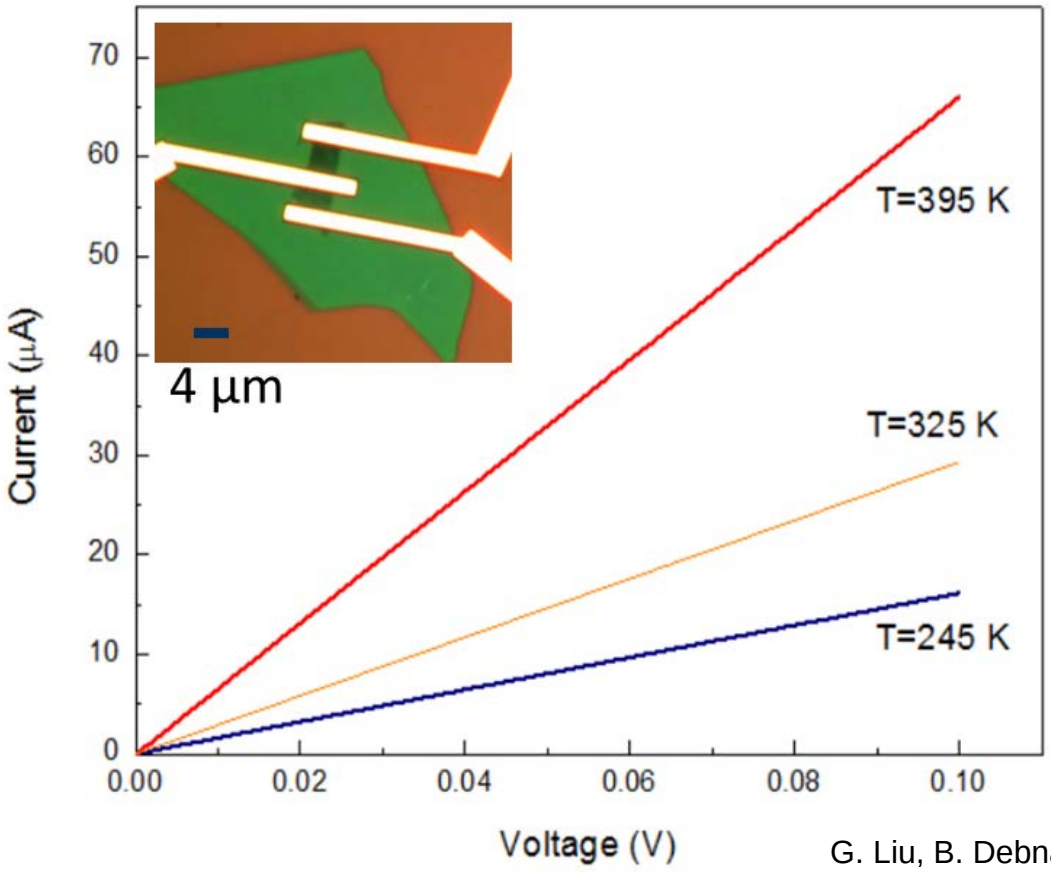

Channel thickness:
t = 6 nm - 9 nm

Contacts:
Pd/Au (15 nm / 60 nm)

→ The h-BN cap provides air stable passivation for the 1T-TaS_2.

→ The edge contacts provide good Ohmic contacts to the 1T-TaS_2.

G. Liu, B. Debnath, T.R. Pope, T.T. Salguero, R.K. Lake and A.A. Balandin, Nature Nanotech, 11, 845 (2016).

I-V Characteristics of Thin Film 1T-TaS_2

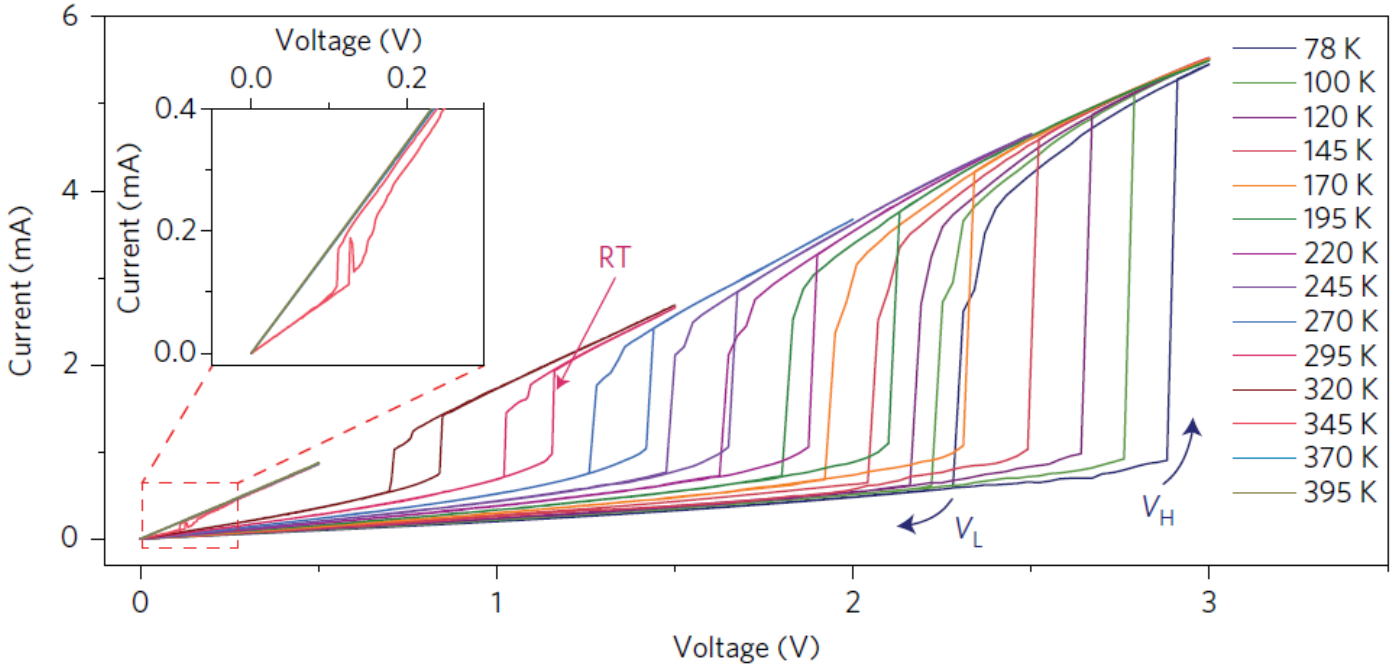

The threshold switching (TS) effect is prominent from 78 K to 320 K. The blues arrows indicate the voltage sweep direction for the measurement at 78 K. For all the other temperatures, V_H is always higher than V_L. The TS is prominent up to 320 K, and becomes less pronounced as the temperature approaches the NC-CDW–IC-CDW transition at 350 K. As shown in the inset, at 345 K (red curve), the TS is still measurable. As T exceeds 350 K, the IV becomes linear.

Low-Voltage I-V Characteristics of Thin Film 1T-TaS_2

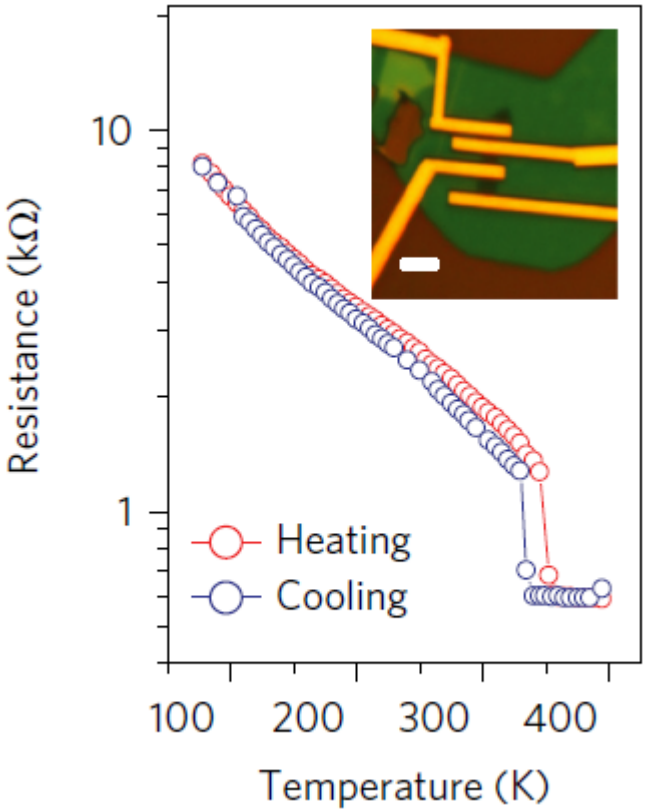

No transition at 180 K

→ Temperature-dependent resistance measurements for 1T-TaS_2. The NC-CDW–IC-CDW and IC-CDW–NC-CDW transitions happen at 350 K and 340 K during the heating and cooling process, respectively. The resistance is measured at low voltage (V=20 mV).

→ Resistances match

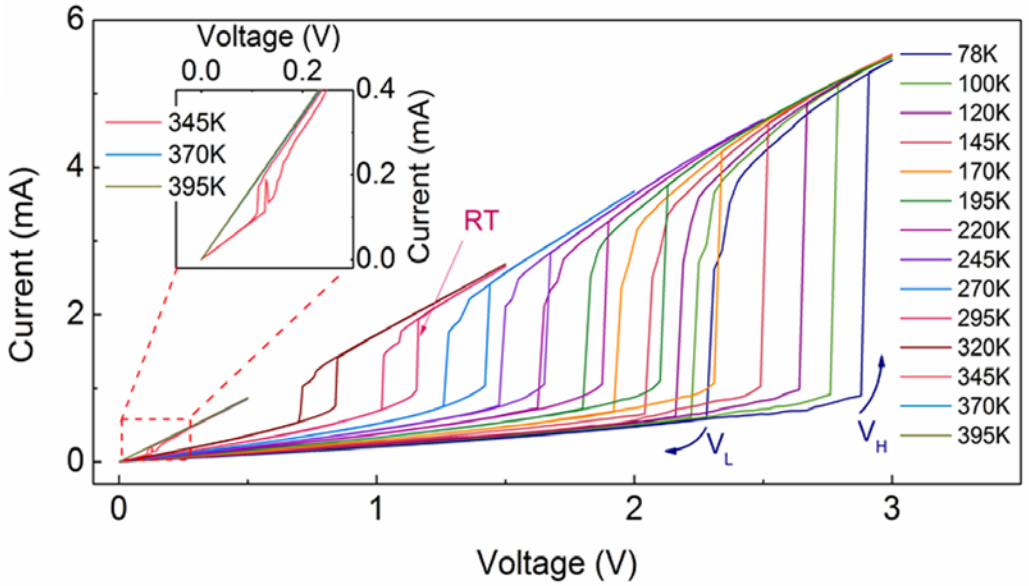

Oscillator Based on 1T-TaS_2 Device

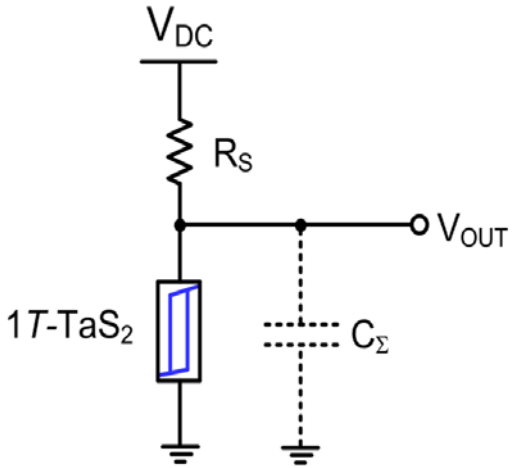

Different operation mechanism from early devices – no de-pinning

Allows for high T operation

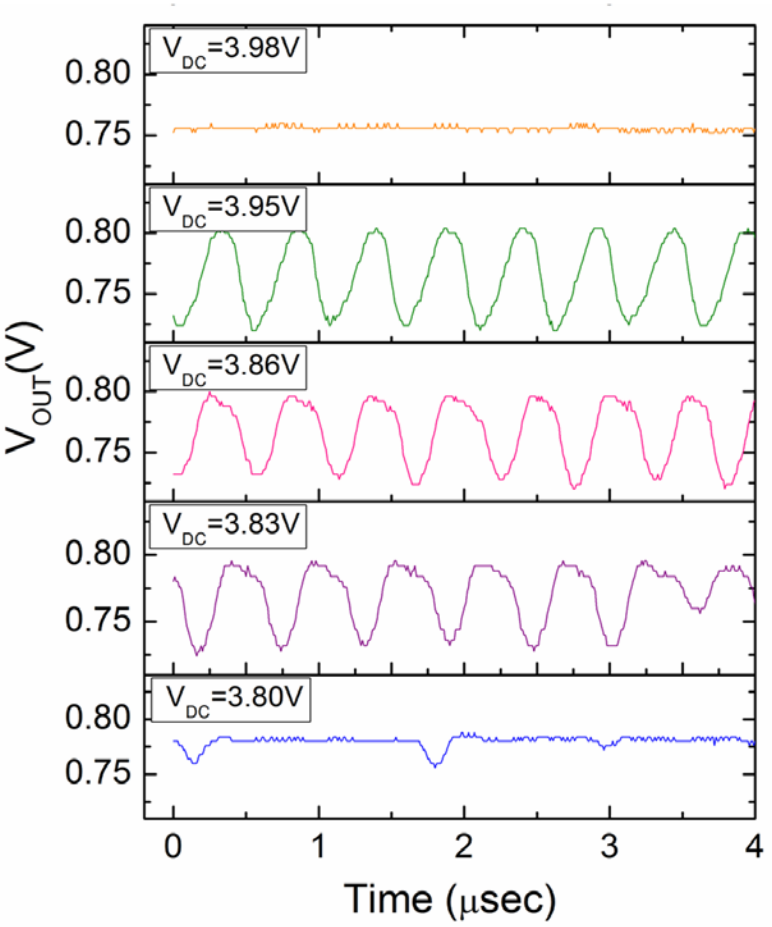

→Circuit schematic of the oscillator consists of the 1T-TaS_2 film, a series connected load resistor, and a lumped capacitance from the output node to ground. The load resistance is 1 kΩ.

→The output terminal is monitored by an oscilloscope.

→Voltage oscillations under different V_{DC}. The circuit oscillates when V_{DC} is within the range of 3.83-3.95 V. The frequency is 1.77 MHz, 1.85 MHz, and 2 MHz when V_{DC} is 3.83, 3.86 and 3.95 V, respectively.

An Integrated 1T-TaS_2 – h-BN – Graphene Oscillator

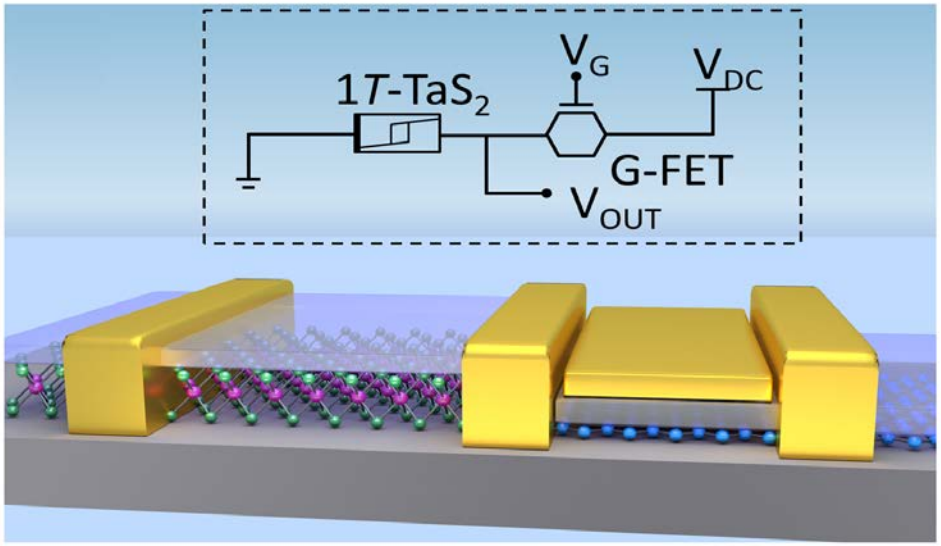

nature nanotechnology
LETTERS
PUBLISHED ONLINE: 4 JULY 2016 | DOI: 10.1038/NNANO.2016.108

A charge-density-wave oscillator based on an integrated tantalum disulfide–boron nitride–graphene device operating at room temperature

Guanxiong Liu[1], Bishwajit Debnath[2], Timothy R. Pope[3], Tina T. Salguero[3], Roger K. Lake[2] and Alexander A. Balandin[1]*

The device structure of the integrated oscillator consists of a graphene FET series connected to 1T-TaS_2.

Both the graphene and TaS_2 are fully covered with h-BN which acts as a protection layer against oxidation for the 1T-TaS_2 and as a gate dielectric for the G-FET.

The equivalent circuit is shown in the inset. The V_{DC} bias is applied at the drain terminal of the G-FET and the V_G bias is connected to the gate terminal of G-FET.

Ground is connected to one terminal of 1T-TaS_2 device, while the common terminal of the two devices is the output port.

G. Liu, B. Debnath, T.R. Pope, T.T. Salguero, R.K. Lake and A.A. Balandin, Nature Nanotech, 11, 845 (2016).

An Integrated 1T-TaS_2 – h-BN – Graphene Oscillator

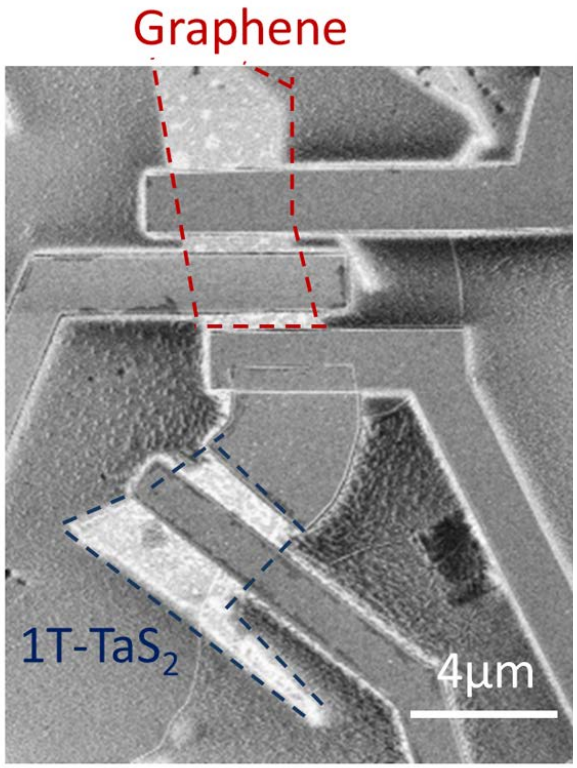

The SEM image of the integrated 1T-TaS_2–BN–graphene voltage controlled oscillator. The graphene and the TaS_2 are highlighted by dashed lines.

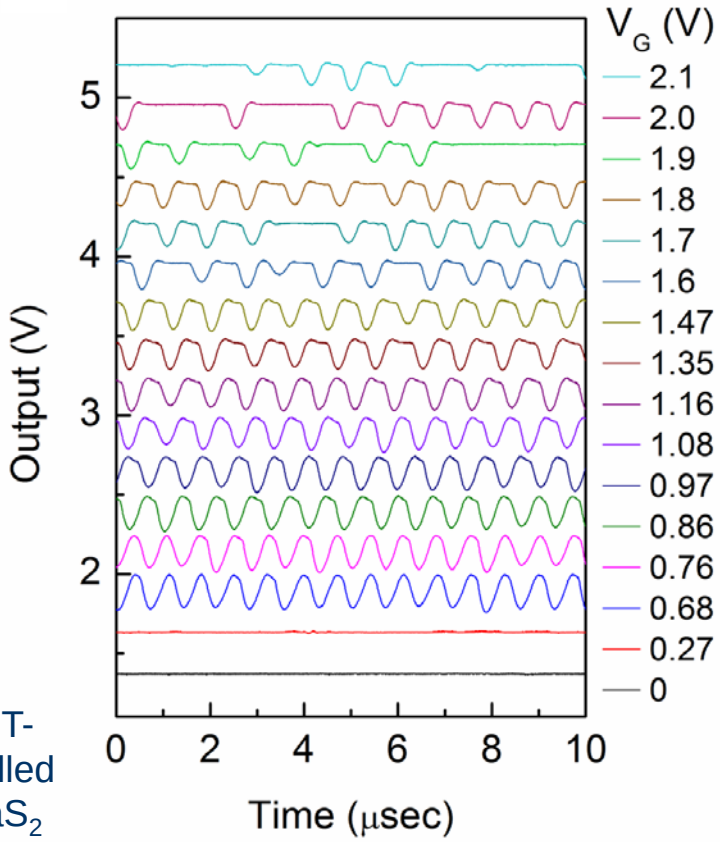

Output waveforms at different gate biases when V_{DC} is fixed at 3.65 V. The oscillation frequency is tunable with gate biases in the range of 0.68 V to 1.8 V. The different waveforms are vertically offset of 0.25 V for clarity.

G. Liu, B. Debnath, T.R. Pope, T.T. Salguero, R.K. Lake and A.A. Balandin, Nature Nanotech, 11, 845 (2016).

An Integrated 1T-TaS_2 – h-BN – Graphene Oscillator

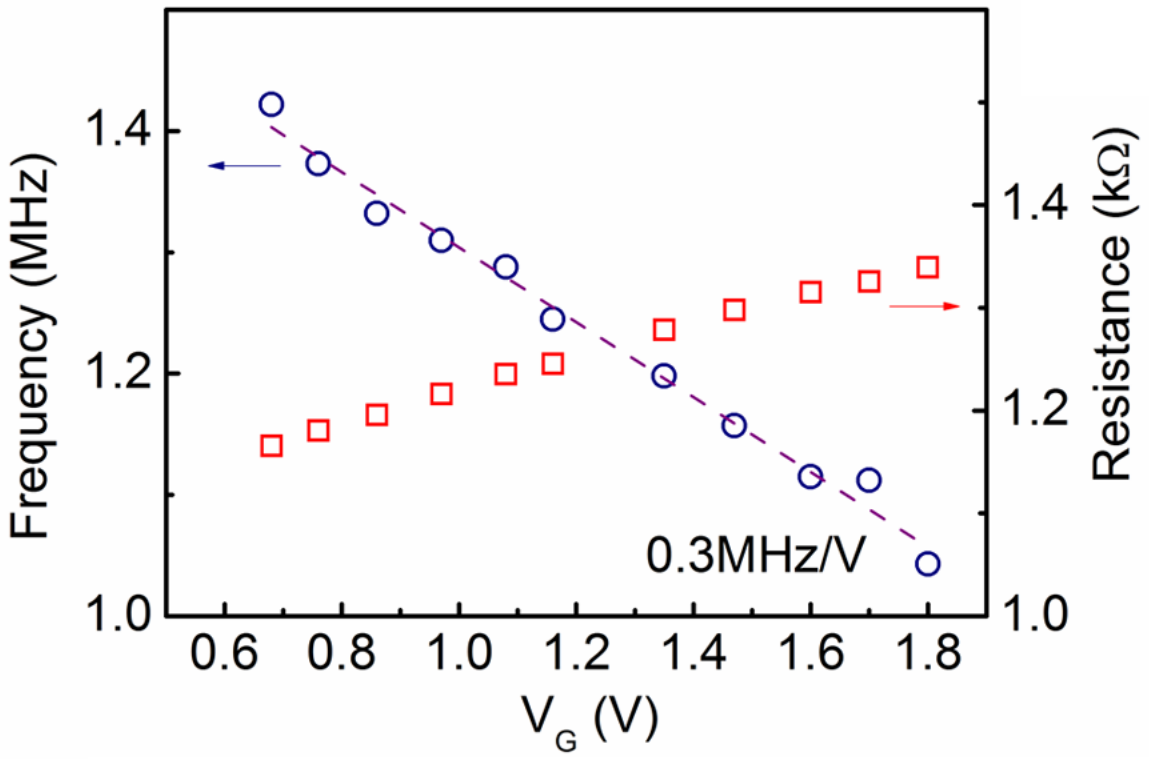

The dependence of oscillation frequency as function of gate bias.

Blue circles show the frequency of the oscillation under increased gate bias. The frequency can be adjusted monotonically with the tuning sensitivity of 0.3M Hz/V.

The red squares are the resistance value of the G-FET under different gate biases with fixed V_{DC}=2.4V.

Circuits Based on CDW Devices

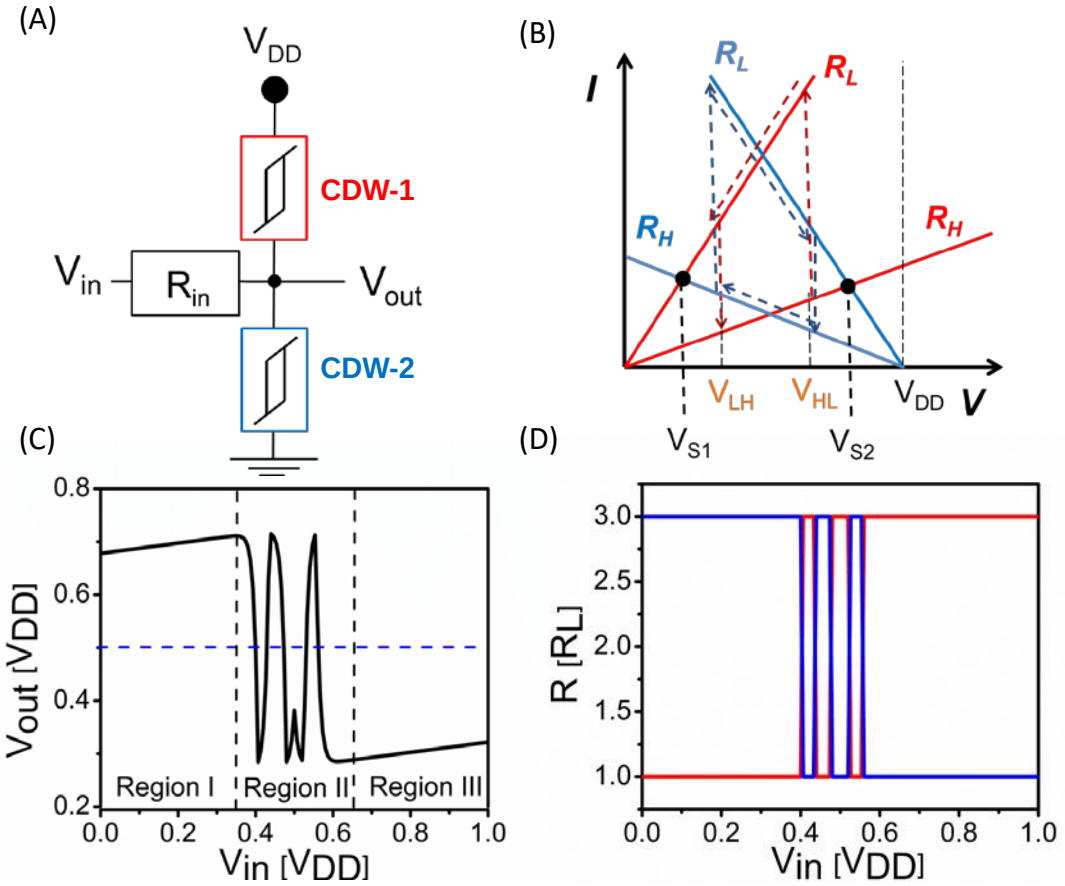

(a) Schematic of the inverter gate consisting of two CDW devices and one regular resistor. (b) Phase space of the circuit comprising two CDW devices. (c) Results of numerical modeling showing the output voltage V_{out} as a function of V_{in}. (d) The change in the CDW resistances R_1 and R_2 as a function of V_{in}.

A. G. Khitun, A. K. Geremew, and A. A. Balandin, “Transistor-less logic circuits implemented with 2-D charge density wave devices,” IEEE Electron Device Lett., vol. 39, no. 9, pp. 1449–1452, 2018.

1T-TaS_2 CDW Devices Under X-Ray Irradiation

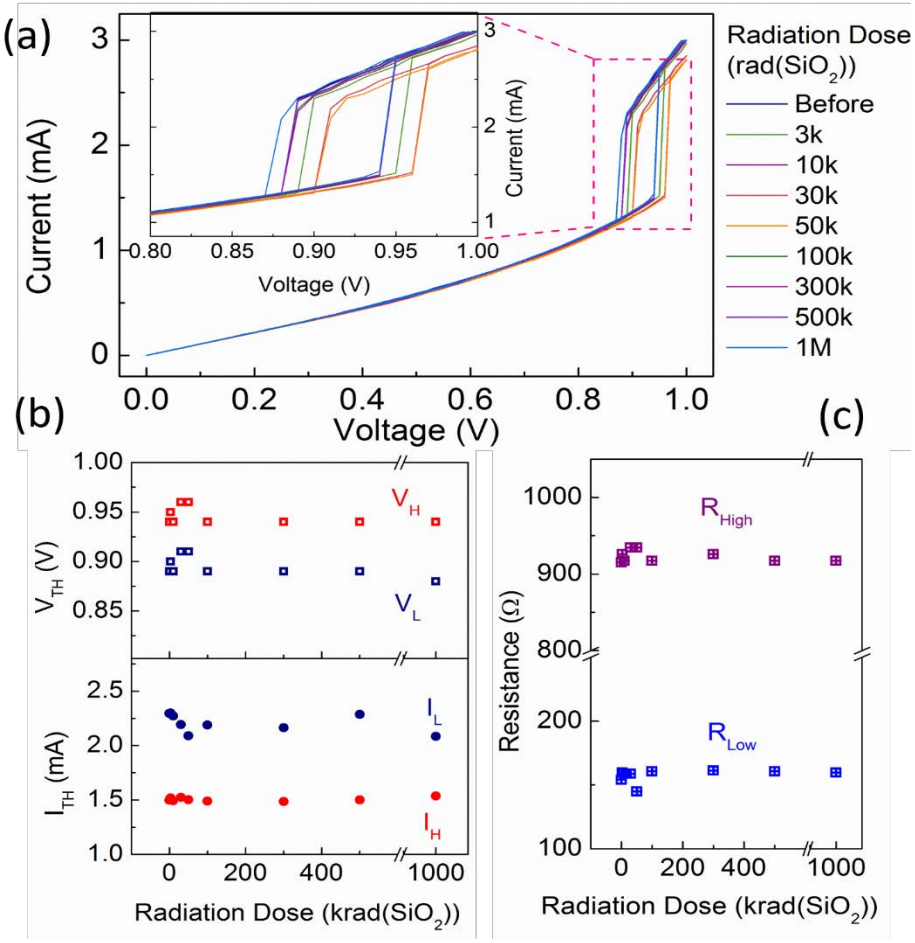

TID response of 1T-TaS_2 devices up to 1 M rad (SiO_2). (a) I-V curves measured after each X-ray irradiation step. (b) Threshold voltages, V_H and V_L, threshold currents, I_H and I_L as function of dose. (c) Extracted resistance at the high resistance and low resistance states as a function of dose.

Carrier concentration:
10^{21} cm^{-2} - 10^{22} cm^{-2}

G. Liu, E. X. Zhang, C. Liang, M. Bloodgood, T. Salguero, D. Fleetwood, A. A. Balandin, "Total-ionizing-dose effects on threshold switching in 1T-TaS_2 charge density wave devices," IEEE Electron Device Letters, 38, 1724 (2017).

Radiation Hardness of CDW Devices

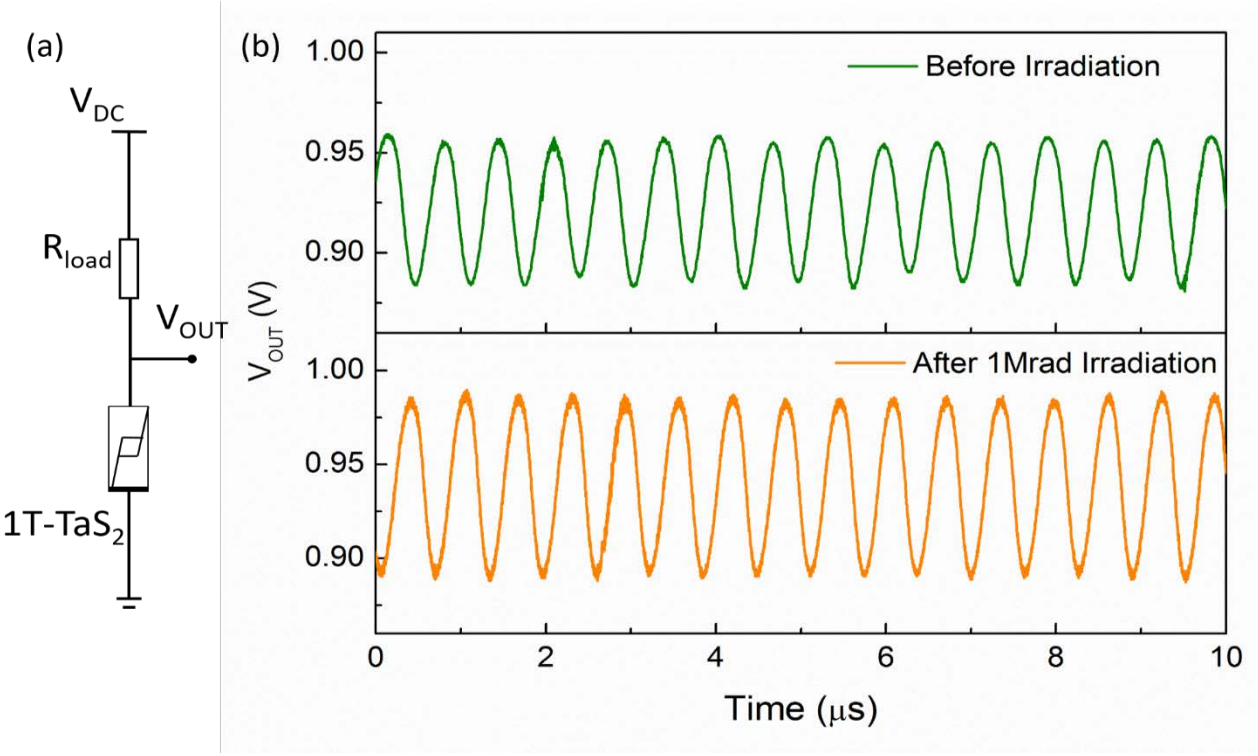

(a) Circuit schematic diagram of a self-sustaining oscillator implemented with one 1T-TaS_2 device and a load resistor. (b) Oscillation waveform before and after 1 Mrad(SiO_2) X-ray irradiation

G. Liu, E. X. Zhang, C. Liang, M. Bloodgood, T. Salguero, D. Fleetwood, A. A. Balandin, "Total-ionizing-dose effects on threshold switching in 1T-TaS_2 charge density wave devices," IEEE Electron Device Letters, 38, 1724 (2017).

Proton Effect on 1T-TaS_2 Devices

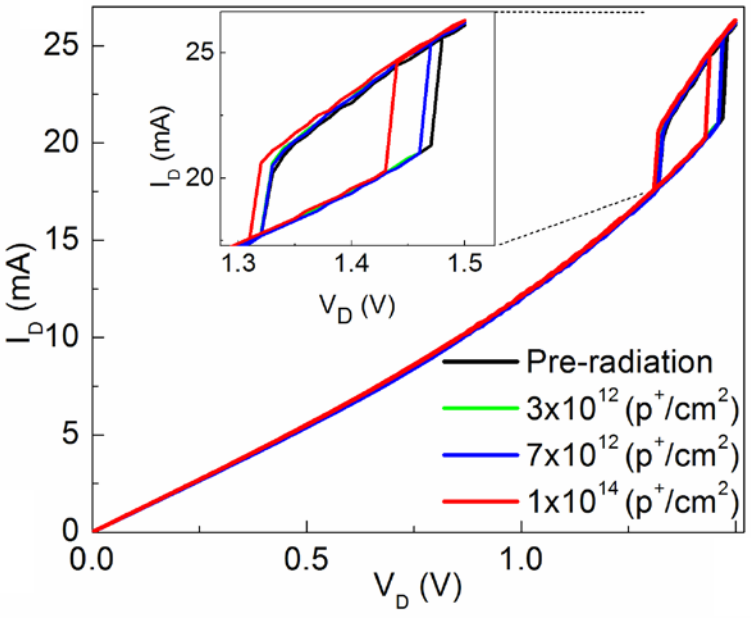

The quasi-two-dimensional (2D) 1T-TaS_2 channels show a *remarkable* immunity to bombardment with the high-energy 1.8 MeV protons to, at least, the irradiation fluence of 10^{14} H^+cm^{-2}.

Collaboration with Vanderbilt University

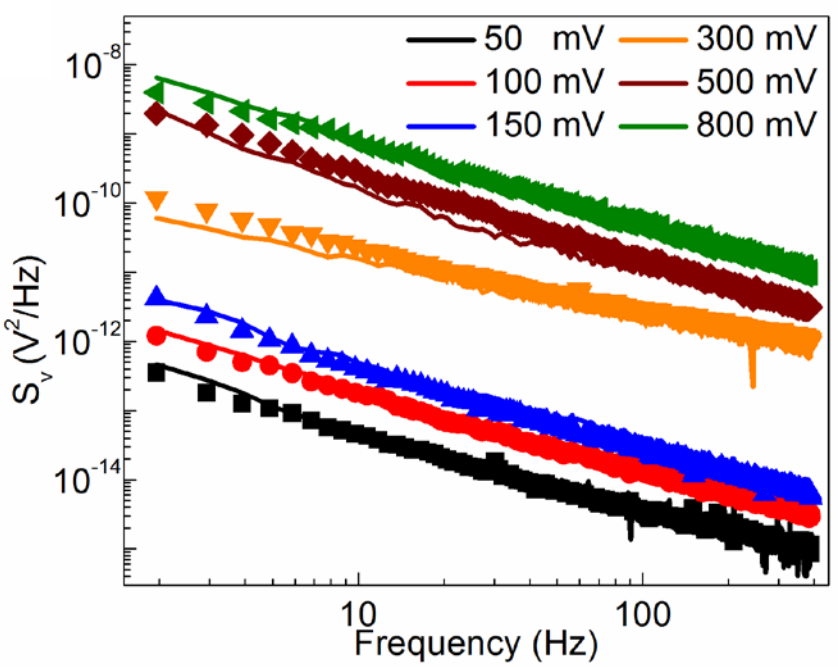

A. Geremew, et al., “Proton-Irradiation-Immune Electronics Implemented with Two-Dimensional Charge-Density-Wave Devices,” Nanoscale, 11, 8380 (2019).

Noise Spectroscopy of CDW Sliding and Transitions

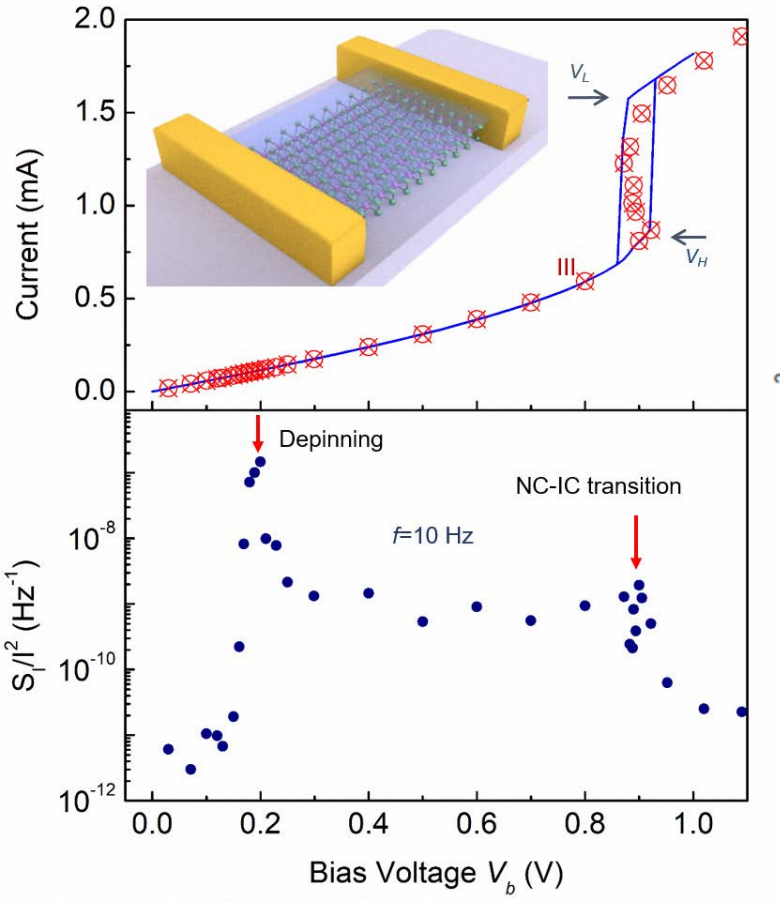

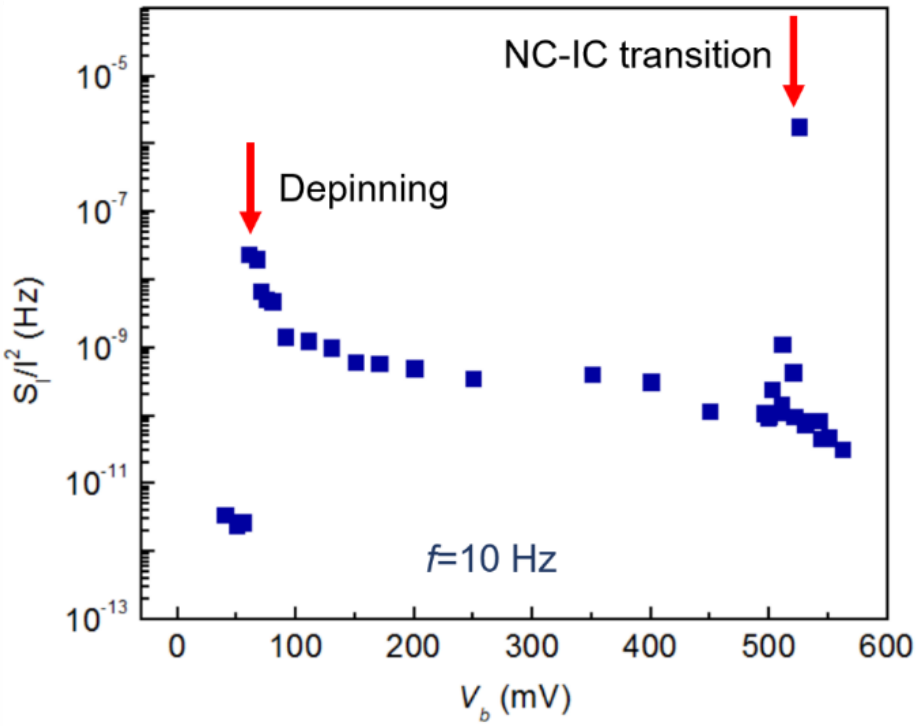

G. Liu, S. Rumyantsev, M. A. Bloodgood, T. T. Salguero, and A. A. Balandin, "Low-frequency current fluctuations and sliding of the charge density waves in two dimensional materials," Nano Letters, 18, 3630 (2018).

Unusual Features of Lorentzian Peaks in Noise of CDWs

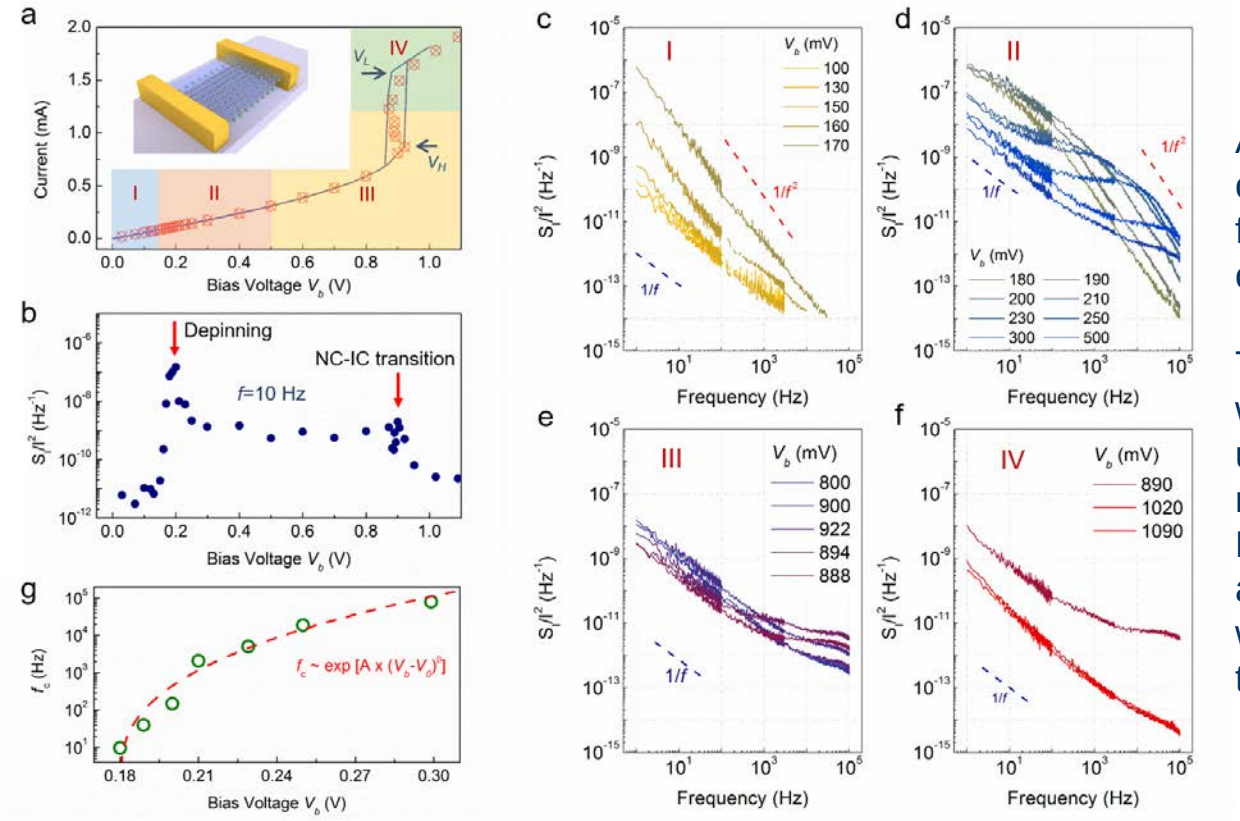

A voltage increase of only 120 mV results in a four orders-of-magnitude change in f_c.

This drastic change in f_c with the bias is highly unusual for conventional materials, where a Lorentzian spectrum is associated G-R noise with f_c independent from the bias.

G. Liu, S. Rumyantsev, M. A. Bloodgood, T. T. Salguero, and A. A. Balandin, "Low-frequency current fluctuations and sliding of the charge density waves in two dimensional materials," Nano Letters, 18, 3630 (2018).

RTS Noise in CDW Devices

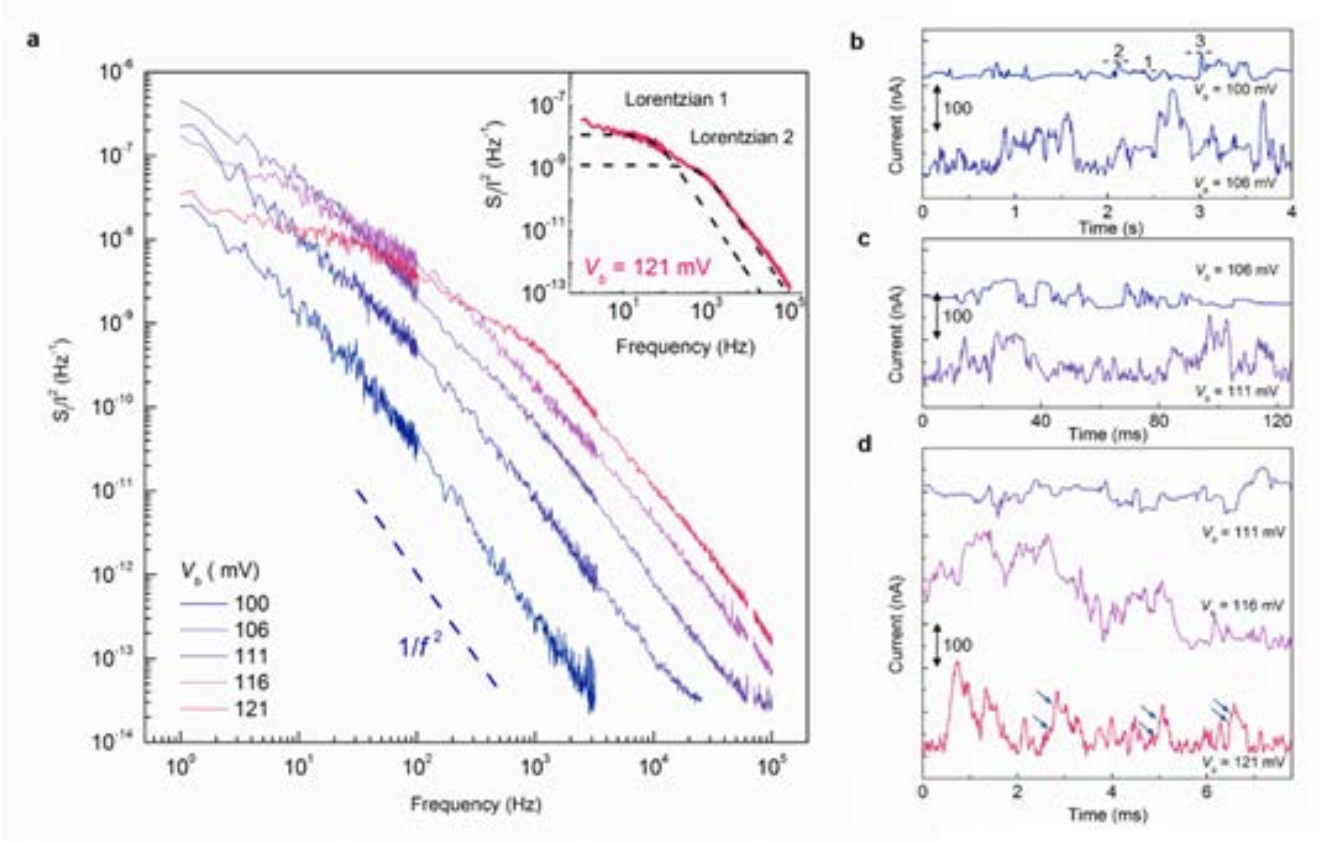

(a) The noise spectral density after onset of sliding at different V_b. The corner frequency increases with increasing V_b.

(b) (c) (d) Time-domain signals at V_b and time scales. Note that a small increase of the bias results in a significant change in the noise. The amplitude of the pulses increases and number of fluctuators becomes lager. This is different from classical RTS noise in semiconductor devices.

G. Liu, S. Rumyantsev, M. A. Bloodgood, T. T. Salguero, and A. A. Balandin, "Low-frequency current fluctuations and sliding of the charge density waves in two dimensional materials," Nano Letters, 18, 3630 (2018).

IC CDW – Metal Transition in Quasi-2D CDW Materials

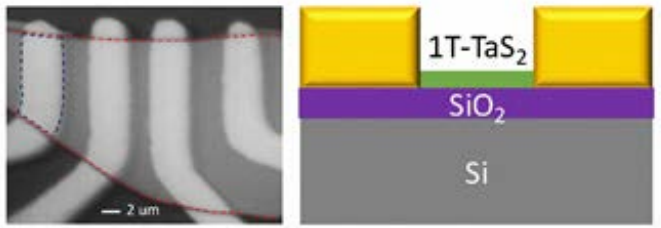

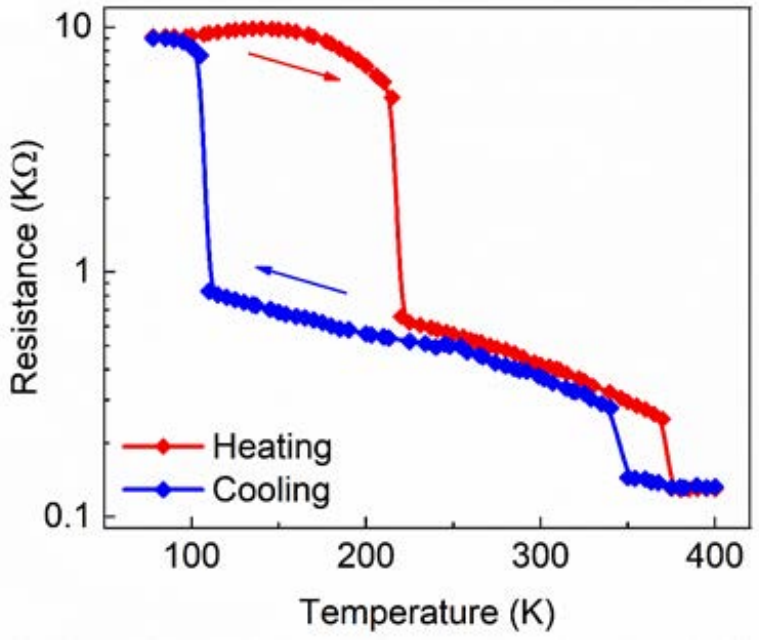

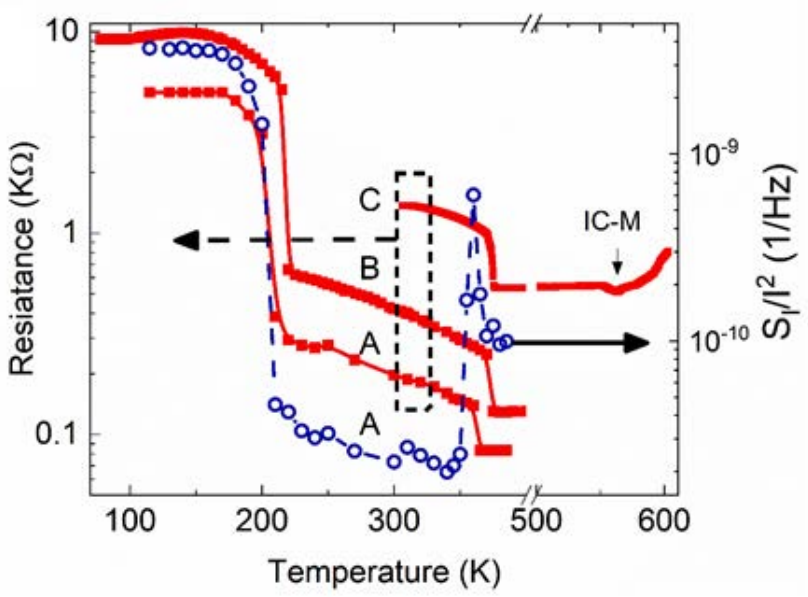

Optical image of a representative device (left panel) and a schematic of the device layered structure (right panel). The scale bar is 2 μm.

A. Geremew, et al., "Bias-Voltage Driven Switching of the Charge-Density-Wave and Normal Metallic Phases in 1T-TaS_2 Thin-Film Devices," ACS Nano (2019).

Noise Spectroscopy of CDW Transitions

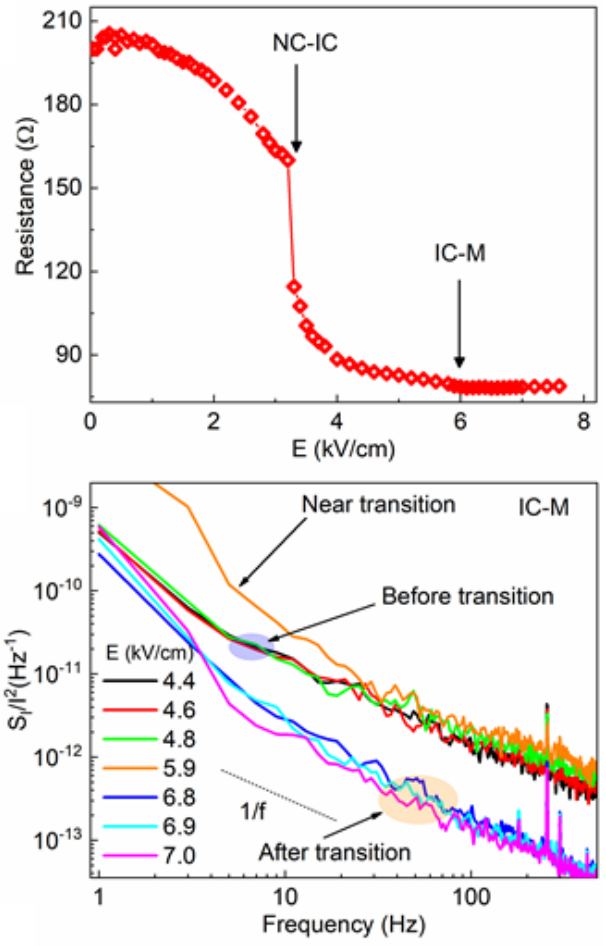

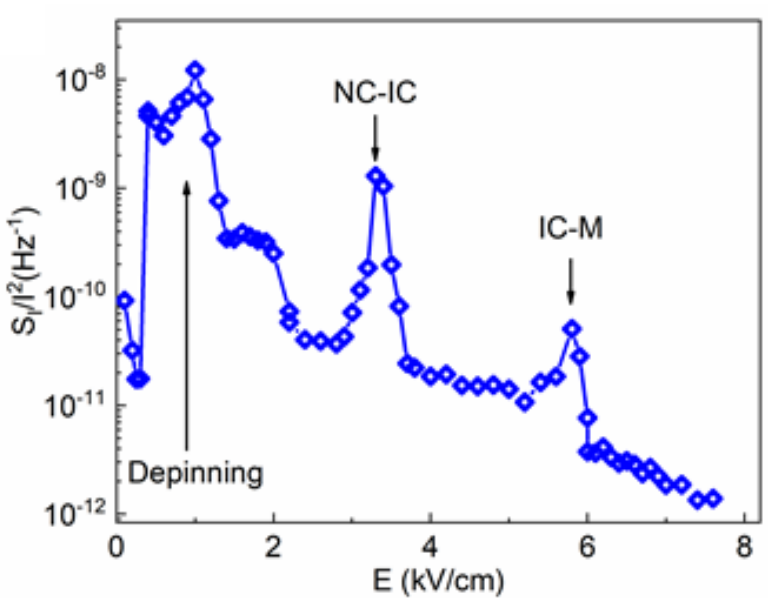

→ Resistance as a function of the applied electric field measured at room temperature.

→ Normalized current noise spectral density as the function of frequency for several values of the electric field, which include the point of transition from the incommensurate CDW to the normal metallic phase.

→ Normalized current noise spectral density, measured at f=10 Hz, as the function of the electric field.

Vertical CDW Devices

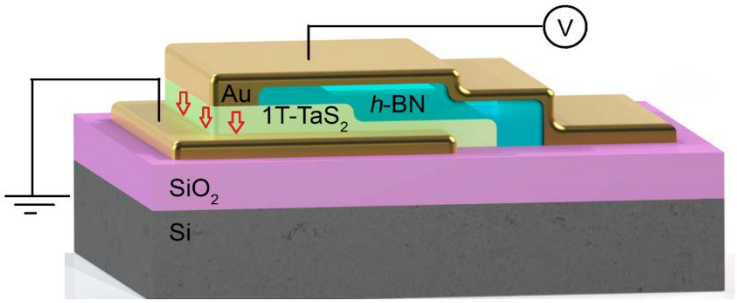

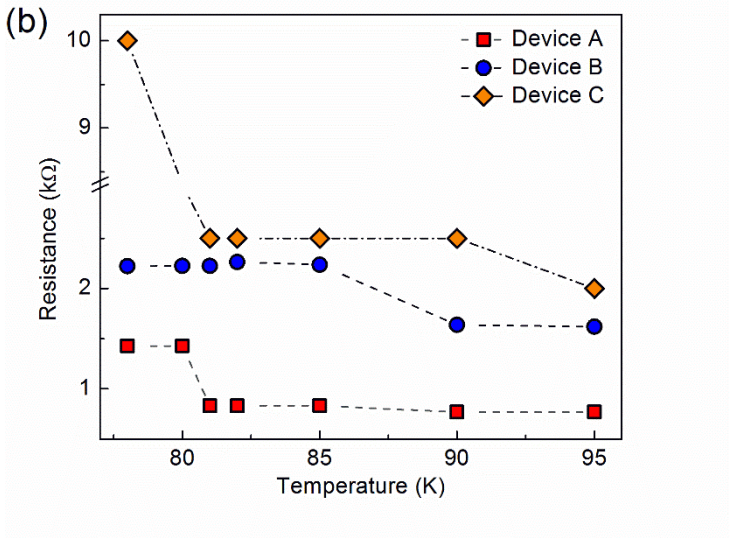

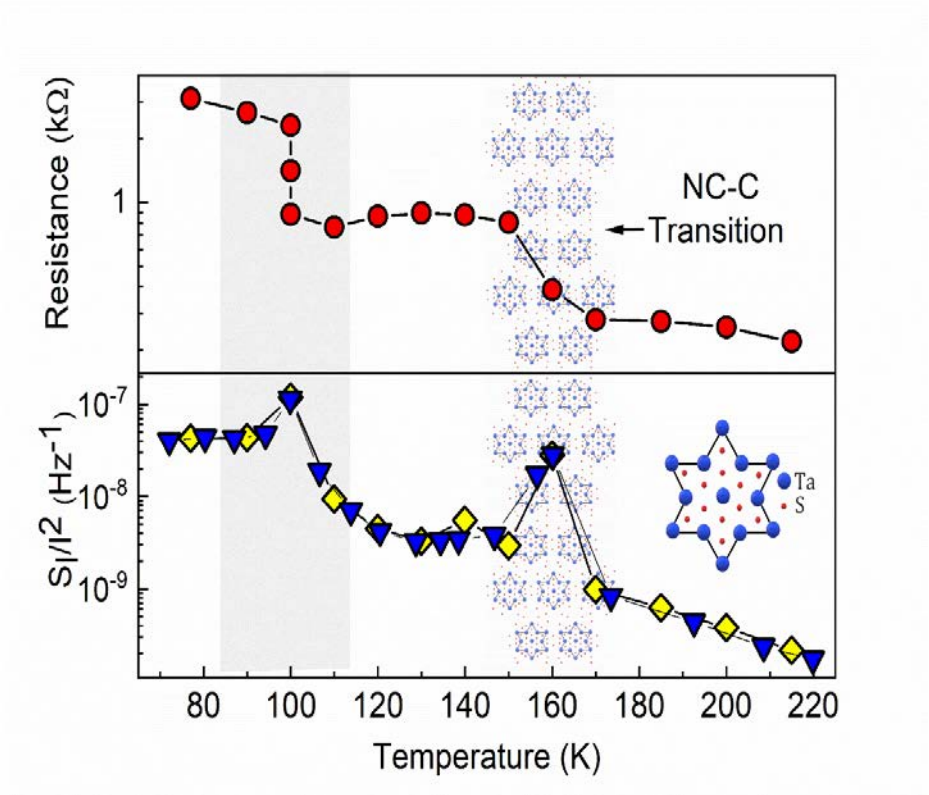

R. Salgado, et al., "Low-frequency noise spectroscopy of charge-density-wave phase transitions in vertical quasi-2D 1T-TaS_2 devices," Applied Physics Express, vol. 18, no. 3, pp. 037001, 2019.

Part – III: 1D Van der Waals Materials

Can we exfoliate Quasi-1D atomic threads like we do quasi-2D atomic planes?

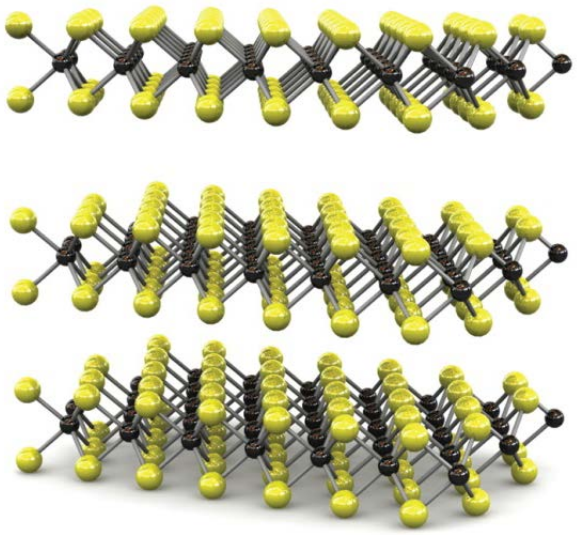

MoS_2

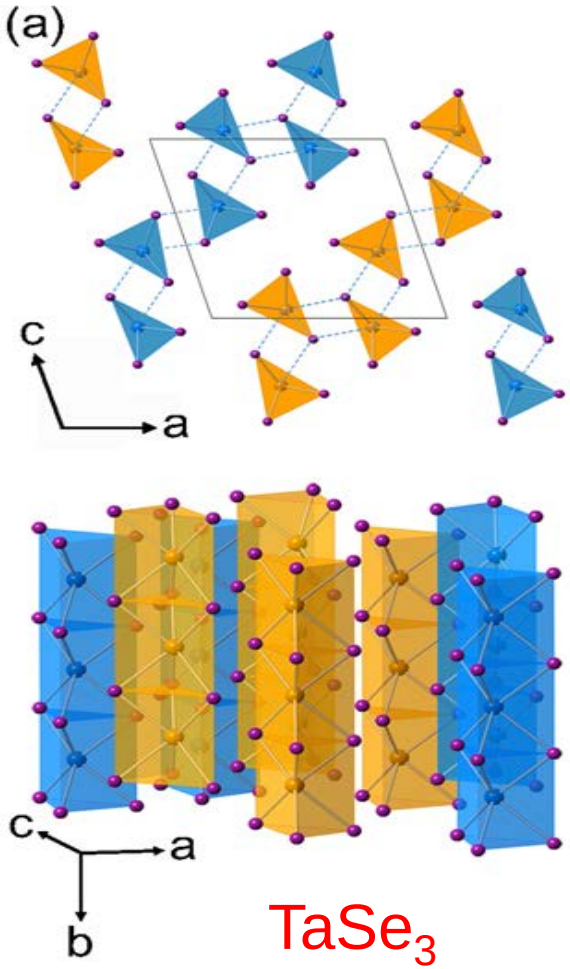

$TaSe_3$

→ Crystal structure of monoclinic $TaSe_3$, with alternating layers of $TaSe_3$

→ Cross section of the unit cell, perpendicular to the chain axis (b axis).

→ The side view: 1D nature of $TaSe_3$ chains along the b axis.

Practical Motivations for the Search of New Interconnect Materials

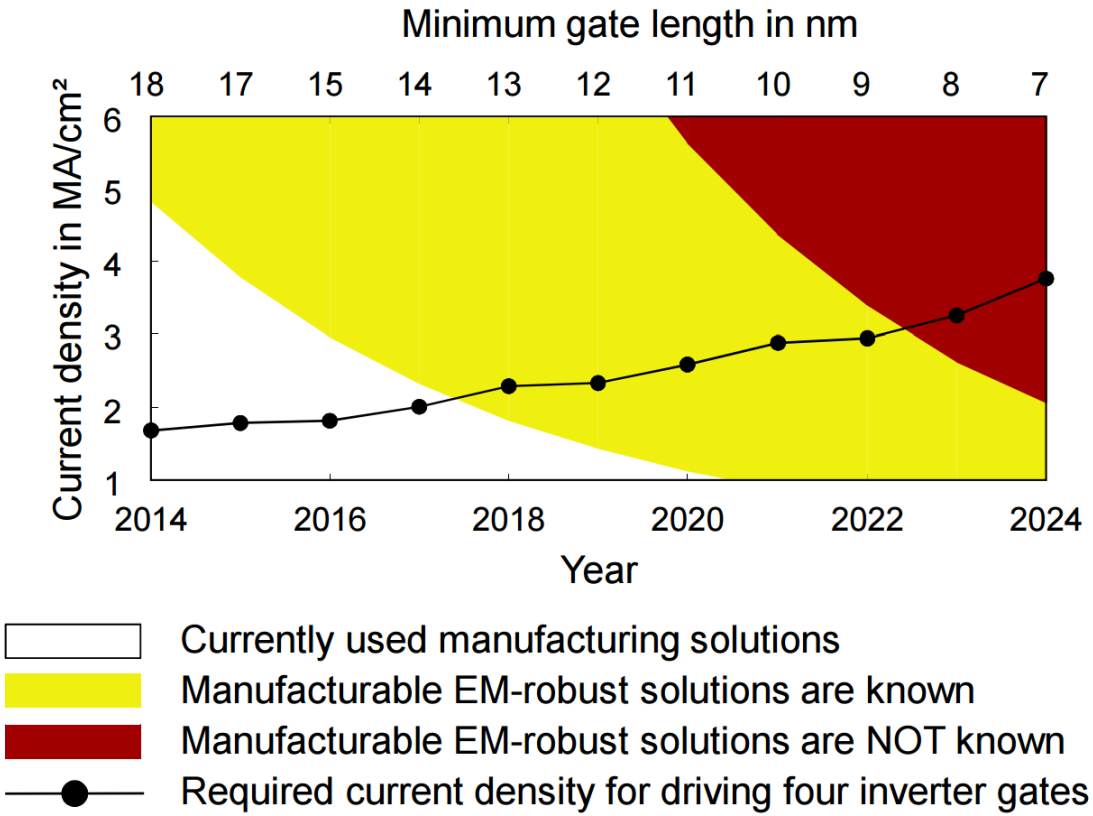

According to ITRS:

→ Current density ~1.8 MA/cm^2 at the half-pitch width of 28.5 nm will increase to ~5.35 MA/cm^2 at the width of 7 nm.

→ There is no existing technology with the breakdown current density high enough to sustain such currents.

→ The layer thicknesses will decrease from 57.0 nm in 2016 to 15.4 nm by 2028

Boron Nitride Capped Devices with Quasi-1D $TaSe_3$ Channels

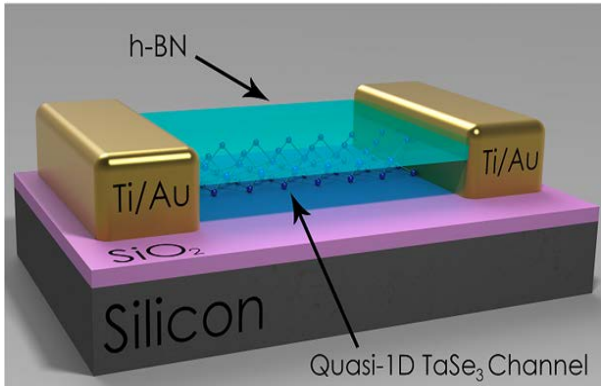

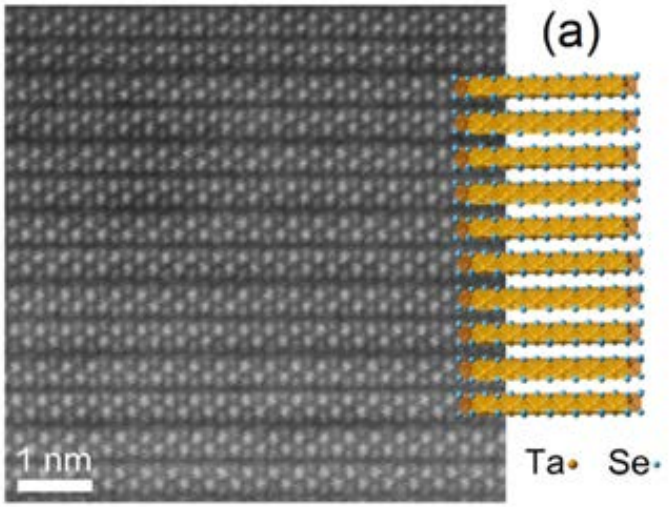

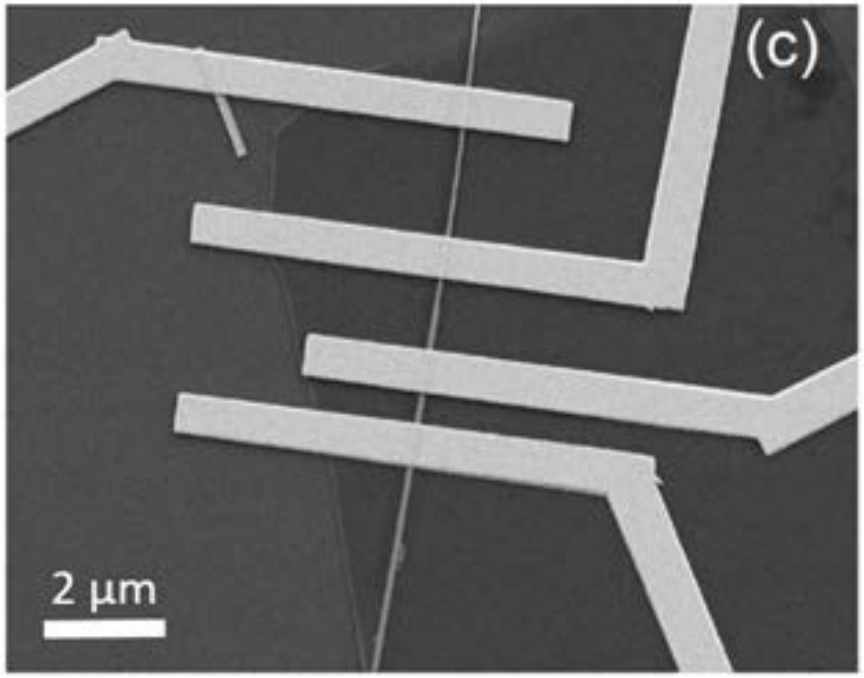

M.A. Stolyarov, G. Liu, M.A. Bloodgood, E. Aytan, C. Jiang, R. Samnakay, T.T. Salguero, D.L. Nika, S.L. Rumyantsev, M.S. Shur, K.N. Bozhilove and A.A. Balandin, Breakdown current density in h-BN-capped quasi-1D $TaSe_3$ metallic nanowires, *Nanoscale*, **8**, 15774 (2016)

Low-Field Electrical Characteristics of Devices with Quasi-1D $TaSe_3$ Channels

- Current-voltage characteristics of $TaSe_3$ devices with different channel length.
- Linear characteristics at low voltage indicates good Ohmic contact of $TaSe_3$ channel with the metal electrodes.

The contact resistance extracted from TLM data is $2R_C$=22 Ω-μm

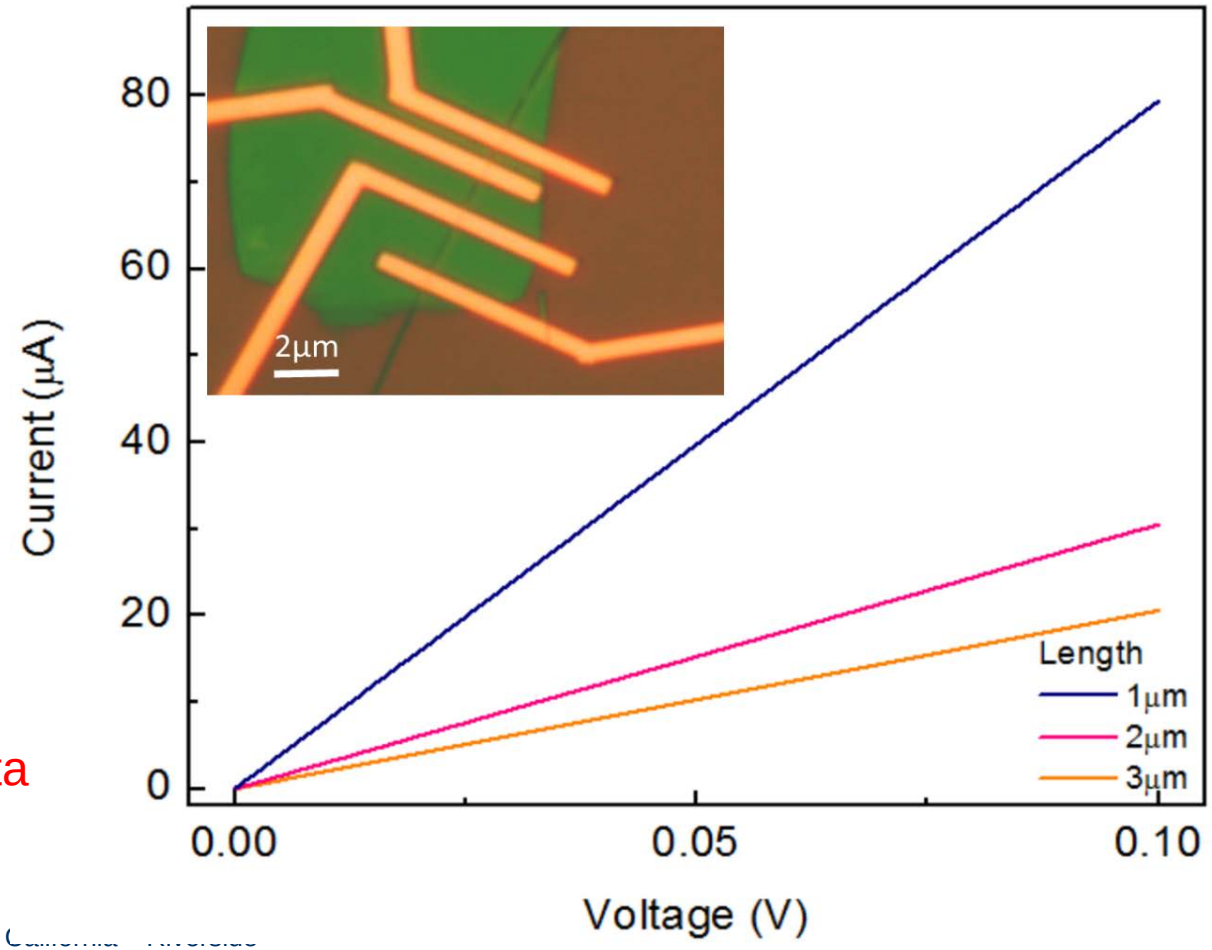

Current Density in Quasi-1D $TaSe_3$ Nanowires

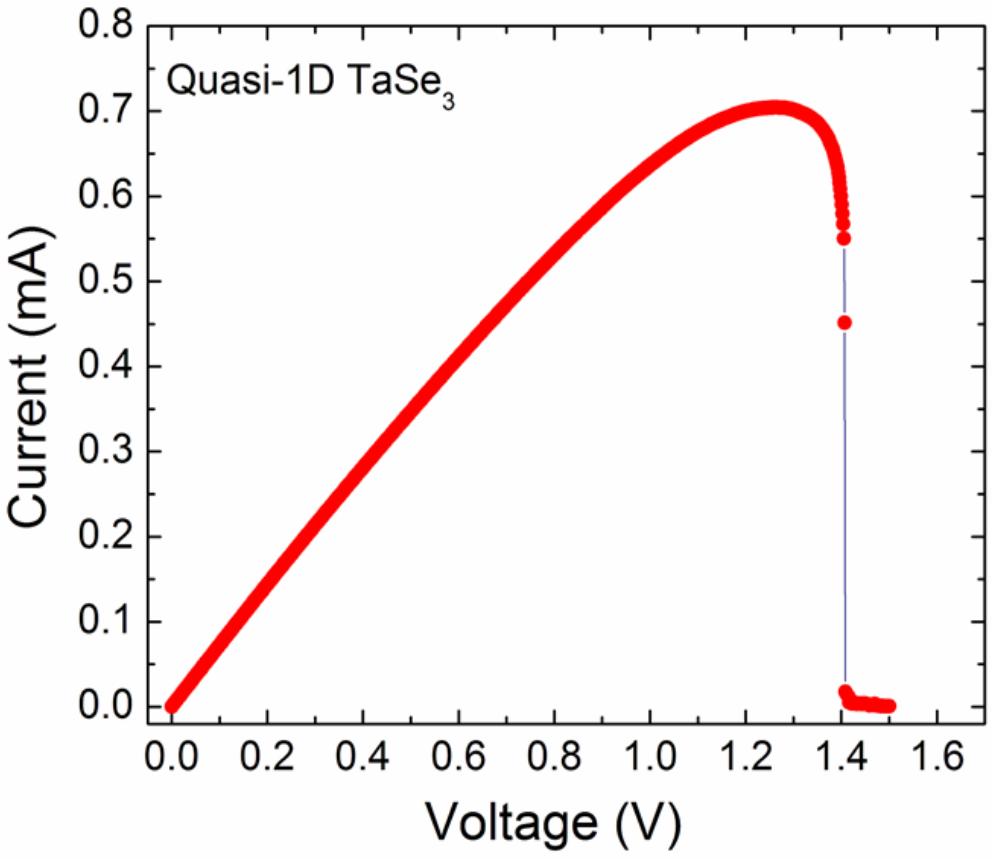

Resistivity is 2.6 – 6.4×10^{-4} Ω-cm.

→ High-field I-V characteristics showing the breakdown point. In this specific device the breakdown is gradual.

→ Breakdown current density of about 32 MA/cm^2 — an order-of-magnitude higher than that for copper.

M.A. Stolyarov, G. Liu, M.A. Bloodgood, E. Aytan, C. Jiang, R. Samnakay, T.T. Salguero, D.L. Nika, S.L. Rumyantsev, M.S. Shur, K.N. Bozhilove and A.A. Balandin, Breakdown current density in h-BN-capped quasi-1D $TaSe_3$ metallic nanowires, *Nanoscale*, **8**, 15774 (2016)

Extracting Electromigration Information from Temperature Dependent Noise Data

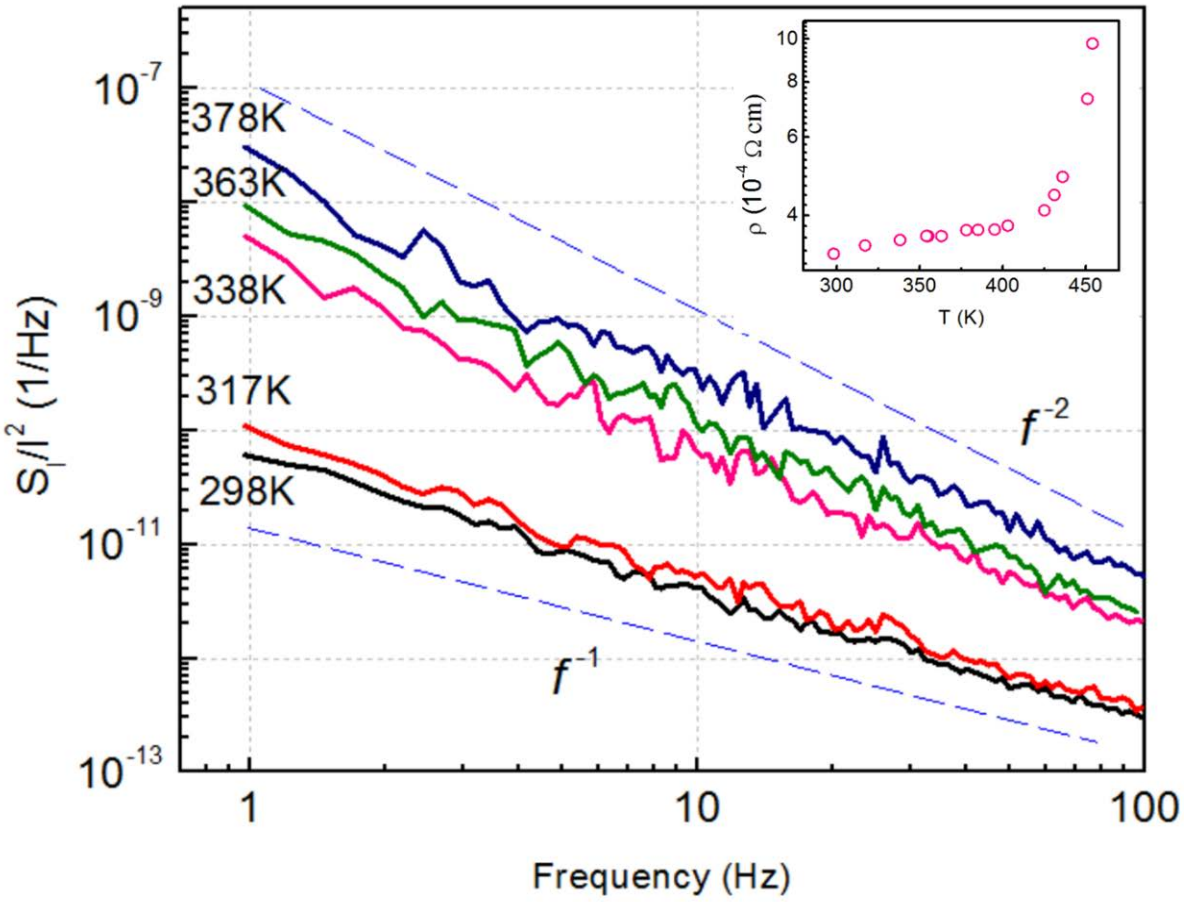

The 1/f noise at RT becomes more of $1/f^2$ – type at elevated temperatures. The increased frequency power factor γ suggests the onset of the electromigration processes.

Inset shows the temperature dependent resistance of the quasi-1D $TaSe_3$ nanowire.

The graduate increase of the resistance with temperature, for T < 410 K is typical for metal. The sharply rising resistance for T > 410 K indicates the occurrence of electromigration.

Noise Analysis: Dutta–Horn Model

Correlation of the frequency power factor γ with the noise (electromigration) activation energy E_P

$$\gamma(T) = 1 - \frac{1}{\ln(2\pi f \tau_0)}\left(\frac{\partial \ln S(f,T)}{\partial \ln T} - 1\right)$$

$$S(f,T) \propto \frac{kT}{2\pi f} D(E)$$

$$E_P = -kT\, ln(2\pi f \tau_0)$$

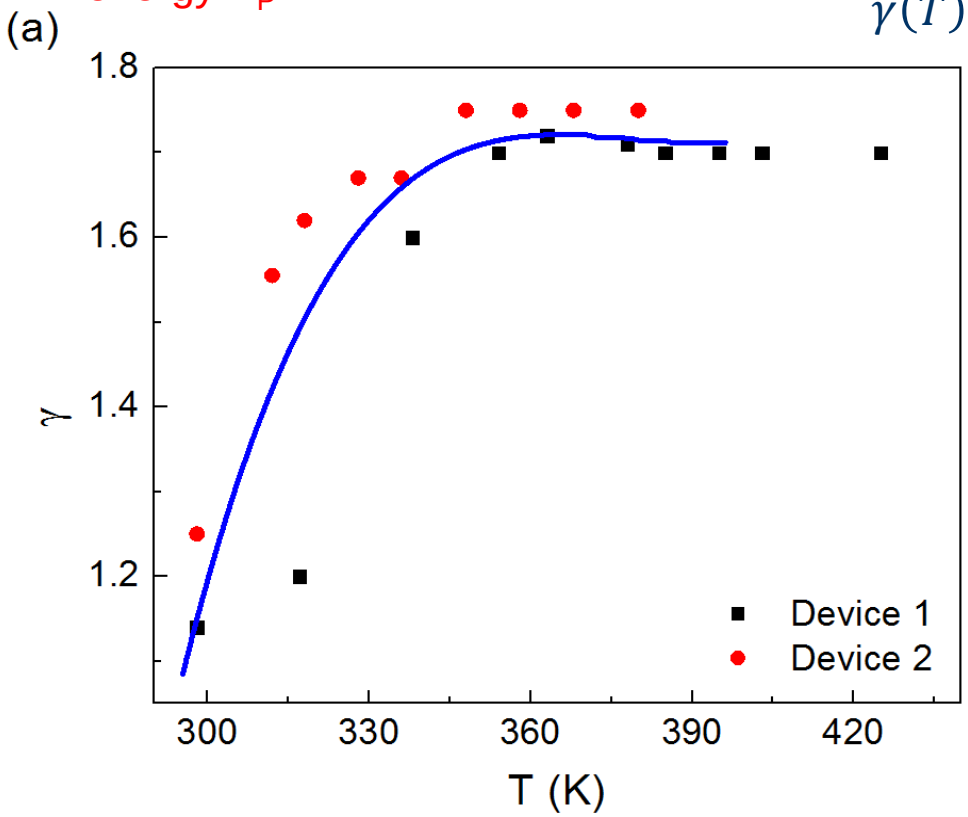

G. Liu, S. Rumyantsev, M. A. Bloodgood, T. T. Salguero, M. Shur, and A. A. Balandin, "Low-frequency electronic noise in quasi-1D $TaSe_3$ van der Waals nanowires," Nano Lett., 17, 377 (2017).

Quasi-1D $ZrTe_3$ van der Waals Nanoribbons

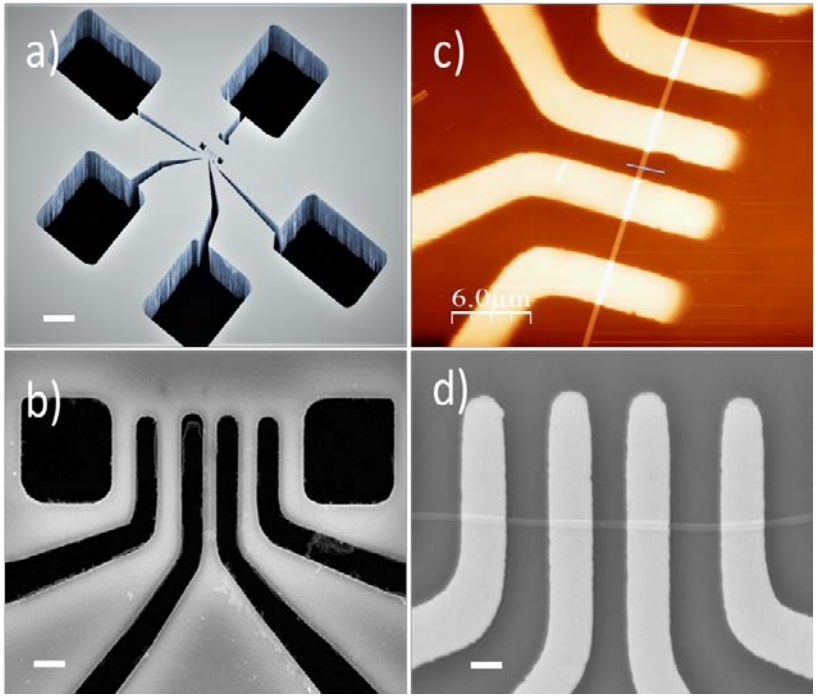

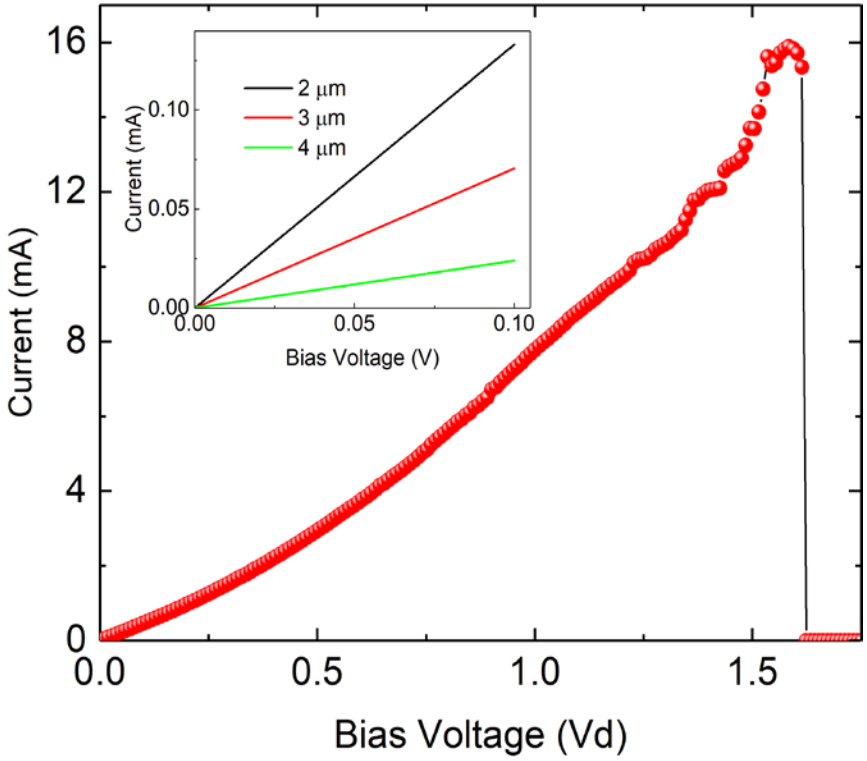

A. Geremew, M. A. Bloodgood, E. Aytan, B. W. K. Woo, S. R. Corber, G. Liu, K. Bozhilov, T. T. Salguero, S. Rumyantsev, M. P. Rao, and A. A. Balandin, "Current Carrying Capacity of Quasi-1D $ZrTe_3$ van der Waals Nanoribbons, IEEE Electron Device Lett., 39, 735 (2018).

Noise Spectroscopy of the $ZrTe_3$ Quasi-1D van der Waals Nanoribbon Devices

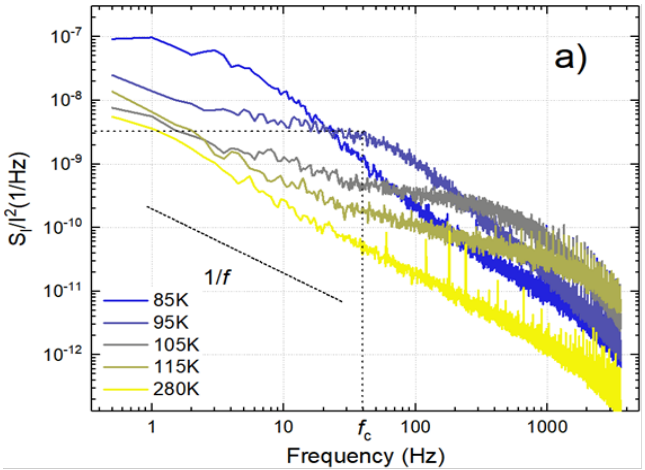

(a) Normalized noise spectral density, S_I/I^2, as a function of frequency of quasi-1D $ZrTe_3$ nanoribbon at temperatures from 85 K to 280 K.

(b) Normalized noise spectral density multiplied by frequency, $S_I/I^2 \times f$, as a function of frequency. Note an unusually strong dependence of the Lorentzian peak on the temperature (at bias 0.1 V)The position of characteristics frequency, *f*c, is shown in broken line.

$$\frac{S_I}{I^2} = \frac{4N_t}{Vn^2}\frac{\tau F(1-F)}{1+(\omega\tau)^2} \qquad \frac{1}{\tau} = \frac{1}{\tau_c} + \frac{1}{\tau_e}$$

$$\tau_c = \frac{1}{\sigma v_T n} \qquad \tau_e = \frac{1}{\sigma v_T N_c \exp\left(-\frac{E_0}{kT}\right)}$$

Trap Activation Energies in $ZrTe_3$ Quasi-1D van der Waals Nanoribbon Devices

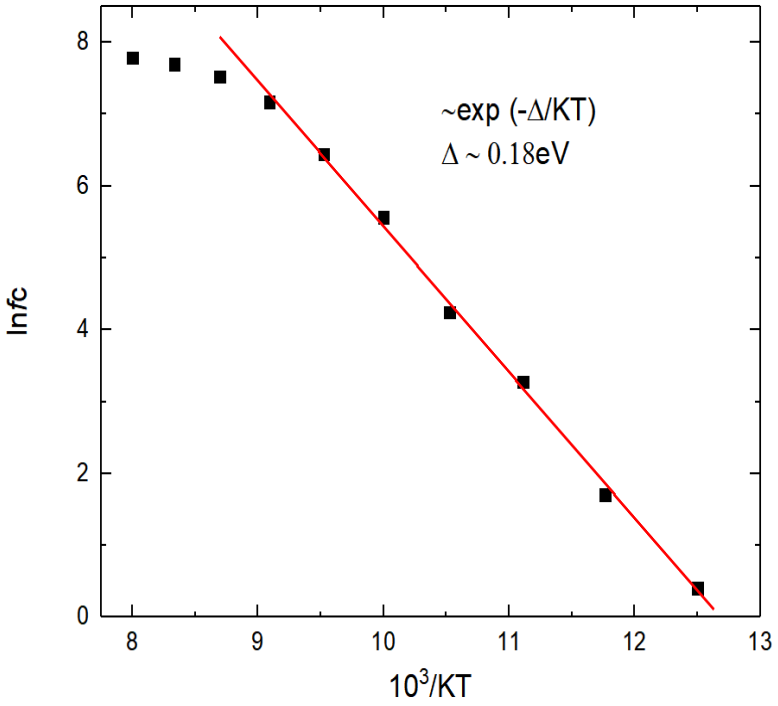

A. K. Geremew, S. Rumyantsev, M. A. Bloodgood, T. T. Salguero, and A. A. Balandin, "Unique features of the generation–recombination noise in quasi-one-dimensional van der Waals nanoribbons," Nanoscale, 10, 19749 (2018).

Arrhenius plot of the characteristics frequency, $\ln(f_c)$, as a function of the inverse of temperature, K^{-1} in quasi-1D $ZrTe_3$ device. This plot was used to extract the activation energy.

The extracted trap activation energy is $E_0 \cong$ 0.18 eV.

$$\sigma = \sigma_0 \exp(-\frac{E_1}{kT}).$$

The activation energy of the cross-section temperature dependence and level position can be easily extracted as E_1=0.144 eV and E_0=0.0456 eV. These data indicate that the activation energy of the characteristic frequencies of the G-R noise peaks is dominated by the activation energy of the capture cross-section.

The Poole-Frenkel Effect or NOT?

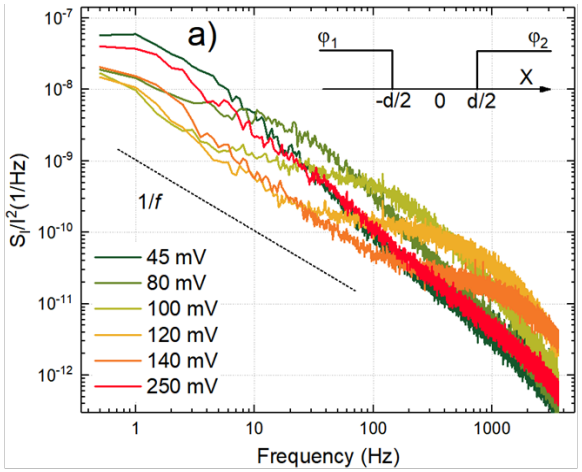

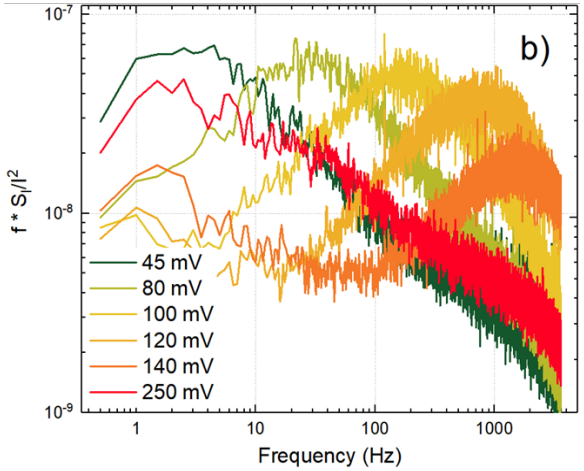

(a) Normalized noise spectral density, S_f/I^2, as a function of frequency of quasi-1D $ZrTe_3$ nanoribbon at the source – drain voltage ranging from 45 mV to 250 mV. Inset shows a schematics of potential barrier height between two states. (b) Normalized noise spectral density multiplied by frequency, $S_f/I^2 \times f$, as a function of frequency. Note an unusually strong dependence of the Lorentzian peak on the source – drain bias (at T =78K).

The shifting of the Lorentzian peak in the noise spectrum with the applied electric field can be due to reducing the impurity barrier potential in high electric field:

$$\Delta E_{fp} = \left(\frac{q^3 F}{\pi \varepsilon_0 \varepsilon}\right).$$

We estimated that the electric filed required to shift this frequency three orders of magnitude is of the order 50 kV/cm. However, for the 2-mm length nanoribbon the average field in the sample does not exceed ~1.25 kV/cm.

$$F\left(\frac{\varphi_1}{x + d/2} - \frac{\varphi_2}{-x + d/2}\right)\frac{1}{\ln L/a}$$

L.D. Landau & E.M. Lifshitz Electrodynamics of Continuous Media (1960)

Conclusions

- → Typical graphene transistors reveal rather low level of the low-frequency noise: $S_I/I^2 = 10^{-9}$ to 10^{-7} Hz^{-1} at f=10 Hz or $A=10^{-9} – 10^{-7}$
- → It is possible to reduce 1/*f* noise via electron beam irradiation
- → Noise reduction after irradiation is better explained by the mobility fluctuation models
- → Low-frequency fluctuations can be used for selective sensing with graphene
- → Demonstrated current density of 10 MA/cm^2 – 30 MA/cm^2 in $TaSe_3$ and up to 100 MA/cm^2 in $ZrTe_3$ nanowires
- → Low-frequency noise measurement is a convenient technique to monitor phase transitions and de-pinning in CDW materials and devices
- → Low-frequency noise was used for extraction activation energies
- → G-R noise reveals unusual behavior in quasi-1D materials

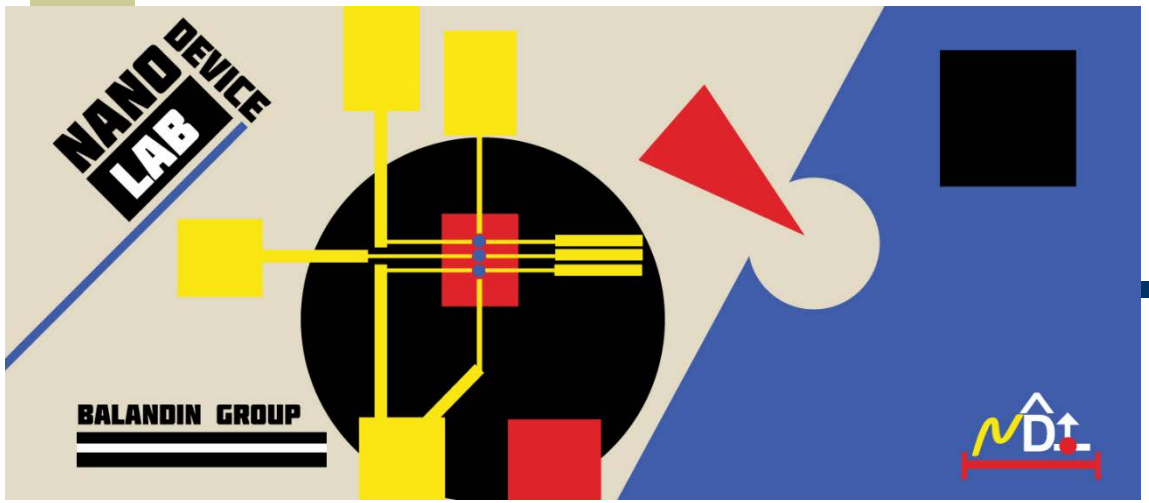
NANO DEVICE LAB
BALANDIN GROUP


NANO-DEVICE LABORATORY